AD_____

AWARD NUMBER: W81XWH-17-1-0652

TITLE: "Temporal Evolution of N-Myc Signaling and Early Targeting of the Neuroendocrine Phenotype in Prostate Cancer"

PRINCIPAL INVESTIGATOR: Drs. David Rickman

RECIPIENT: David Rickman, Himisha Beltran

REPORT DATE: Oct 2019

TYPE OF REPORT: Annual

PREPARED FOR: U.S. Army Medical Research and Materiel Command
Fort Detrick, Maryland 21702-5012

REPORT DOCUMENTATION PAGE

Form Approved
OMB No. 0704-0188

1. REPORT DATE	2. REPORT TYPE	3. DATES COVERED
Oct 2019	Annual	30 Sep 2018-29 Sep 2019

4. TITLE AND SUBTITLE

Temporal Evolution of N-Myc Signaling and Early Targeting of the Neuroendocrine Phenotype in Prostate Cancer

5a. CONTRACT NUMBER

5b. GRANT NUMBER
W81XWH-17-1-0652

5c. PROGRAM ELEMENT NUMBER

6. AUTHOR(S)
Dr. David Rickman

Email: dsr2005@med.cornell.edu

5d. PROJECT NUMBER

5e. TASK NUMBER

5f. WORK UNIT NUMBER

7. PERFORMING ORGANIZATION NAME(S) AND ADDRESS(ES)

Weill Medical College of Cornell University

New York, NY 10065

8. PERFORMING ORGANIZATION REPORT NUMBER

9. SPONSORING / MONITORING AGENCY NAME(S) AND ADDRESS(ES)
U.S. Army Medical Research and Materiel Command
Fort Detrick, Maryland 21702-5012

10. SPONSOR/MONITOR'S ACRONYM(S)

11. SPONSOR/MONITOR'S REPORT NUMBER(S)

12. DISTRIBUTION / AVAILABILITY STATEMENT
Approved for Public Release; Distribution Unlimited

13. SUPPLEMENTARY NOTES

14. ABSTRACT

Transformation of castration resistant prostate cancer (CRPC) towards androgen signaling independence has emerged as a resistance mechanism in a subset of metastatic CRPC following exposure to androgen receptor (AR)-targeted therapies such as abiraterone or enzalutamide. Clinically, patients typically present with progression in the setting of a low or modestly rising serum prostate specific antigen (PSA) and metastatic biopsies can show pathologic or molecular features consistent with neuroendocrine prostate cancer (NEPC). NEPC is associated with low or absent AR expression, suppressed AR signaling, retention of early genomic mutations from its adenocarcinoma precursor, and acquisition of distinct genomic and epigenomic alterations (Beltran H, et al, Nature Medicine, 2016). The development of novel therapeutic approaches for patients with NEPC represents a clinical unmet need. Over the last seven years, our group has focused on characterizing the molecular landscape of NEPC and have identified and validated new therapeutic targets, including the N-Myc/Aurora A pathway and specific epigenetic modifiers such as (Enhancer of Zeste Homolog 2) EZH2 (Beltran H, Rickman DS et al Cancer Discovery 2011; Dardenne E, Beltran H, …. and Rickman DS, Cancer Cell 2016).

15. SUBJECT TERMS

16. SECURITY CLASSIFICATION OF:			17. LIMITATION OF ABSTRACT	18. NUMBER OF PAGES	19a. NAME OF RESPONSIBLE PERSON
a. REPORT	b. ABSTRACT	c. THIS PAGE			19b. TELEPHONE NUMBER *(include area code)*
U	U	U	UU		

USAMRMC

TABLE OF CONTENTS

1. **INTRODUCTION:** Narrative that briefly (one paragraph) describes the subject, purpose and scope of the research.

Transformation of castration resistant prostate cancer (CRPC) towards androgen signaling independence has emerged as a resistance mechanism in a subset of metastatic CRPC following exposure to androgen receptor (AR)-targeted therapies such as abiraterone or enzalutamide. Clinically, patients typically present with progression in the setting of a low or modestly rising serum prostate specific antigen (PSA) and metastatic biopsies can show pathologic or molecular features consistent with neuroendocrine prostate cancer (NEPC). NEPC is associated with low or absent AR expression, suppressed AR signaling, retention of early genomic mutations from its adenocarcinoma precursor, and acquisition of distinct genomic and epigenomic alterations (Beltran H, et al, Nature Medicine, 2016). The development of novel therapeutic approaches for patients with NEPC represents a clinical unmet need. Over the last nine years, our group has focused on characterizing the molecular landscape of NEPC and have identified and validated new therapeutic targets, including the N-Myc/Aurora A pathway and specific epigenetic modifiers such as (Enhancer of Zeste Homolog 2) EZH2 (Beltran H, Rickman DS et al Cancer Discovery 2011; Dardenne E, Beltran H, …. and Rickman DS, Cancer Cell 2016).

Hypothesis: *N-Myc is an early driver of the NEPC phenotype, and that by tracking N-Myc signaling during the transition from adenocarcinoma to NEPC, we can identify cooperating factors that promote NEPC progression and define appropriate time points for early intervention.*

To address this hypothesis we formulated 3 Specific Aims:

Specific Aim 1: To assess the timing of N-Myc activation in patients and define how N-Myc and NEPC signaling impacts prognosis. The working hypothesis of this **Aim** is that there are specific molecular changes that serve as early markers of tumors that will evolve to NEPC. We will assess patient tumors at various timepoints during disease progression from prostate adenocarcinoma to NEPC and correlate N-Myc expression and NEPC signaling with clinical features and outcomes. We will also investigate MYCN and AURKA genomic amplification in tumors and circulating tumor DNA (ctDNA). Specifically we will evaluate: 1) localized prostate cancer patients treated with prostatectomy (see **letter of Support, GenomeDx**); 2) high risk localized patients treated with or without neoadjuvant docetaxel and androgen deprivation therapy (NCT00430183); 3) patients with metastatic CRPC treated with abiraterone, and enzalutamide (IRB1305013903, PI Beltran); 4) NEPC patients treated with the Aurora A inhibitor MLN8237 (NCT01799278, PI Beltran). Gene expression will be quantified using a custom-designed assay validated by our group and amenable to FFPE tissues. N-Myc, Aurora A, and AR signaling genes, stem cell, neuronal, and other NEPC markers will be assessed. AURKA and MYCN amplification will be evaluated in tumors and ctDNA by targeted exome sequencing and/or FISH. We predict that N-Myc/NEPC signaling may be detected early in a subset of high-risk patients and this represents the presence of treatment resistant cells, and that this signaling program is enhanced after both short and long term AR-targeted therapies. The detection and determination of the frequency of early NEPC-associated alterations will help molecularly define subsets of prostate adenocarcinomas as harbingers of NEPC. This has clinical implications towards the development of diagnostic, prognostic, and predictive biomarkers to be evaluated early (potentially at the time of prostate cancer diagnosis) to select individuals at high risk for progression for early intervention. These results will also help identify patients less likely to benefit from AR-targeted strategies and more likely to benefit from MLN8237 or other N-Myc directed approaches.

Specific Aim 2: To assess the impact of timing of N-Myc expression on the development of castration resistance and the NEPC phenotype. The working hypothesis of this **Aim** is that N-Myc drives the trans-differentiation of castration resistant adenocarcinomas towards the NEPC phenotype. In order to model the evolutionary acquisition of N-Myc signaling during prostate cancer progression, we will temporally regulate N-Myc expression either at (3 months) or after (6 months and 9 months) the time of disease onset following Pten deletion both in intact mice and

in mice castrated at 6 months. We will to monitor Pten mutant cells (using YFP) before N-Myc and after N-Myc (Td-Tomato) overexpression and lineage trace emerging clones that develop histological and molecular features of NEPC. We expect that castration will lead to a quicker N-Myc-induced onset of NEPC.

Specific Aim 3: To evaluate the influence of N-Myc timing on response to NEPC directed therapeutics. The working hypothesis of this **Aim** is that N-Myc over-expression sensitizes CRPC to NEPC-directed therapeutics. We will test N-Myc-early and N-Myc-late models with drugs that have demonstrated efficacy against NEPC including Aurora kinase A inhibition, platinum chemotherapy and EZH2 inhibitors. We will also evaluate the effect of the EZH2 inhibitors as priming agents with Aurora-A or AR-directed therapies (enzalutamide) in delaying or reversing AR-independent resistance *in vitro* and *in vivo*. We predict that early N-Myc expression results in comparable response to N-Myc targeted therapies as NEPC and early treatment with these agents modulates NEPC transcriptional programs. Results from this **Aim** will aid in biomarker selection for future trials.

2. **KEYWORDS:** Provide a brief list of keywords (limit to 20 words).

Castration resistant prostate cancer (CRPC), androgen receptor (AR)-targeted therapy, neuroendocrine prostate cancer (NEPC), N-Myc transcription factor (N-Myc), Polycomb Repressive Complex 2-associated protein Enhancer of Zeste Homolog 2 (EZH2).

3. **ACCOMPLISHMENTS:** The PI is reminded that the recipient organization is required to obtain prior written approval from the awarding agency Grants Officer whenever there are significant changes in the project or its direction.

What were the major goals of the project?

a. Major goals of the project

1. Specific Aim 1: To assess the timing of N-Myc activation in patients and define how N-Myc signaling impacts response to aurora kinase A inhibition and clinical outcomes.
    a. Evaluate localized prostate cancer patients treated with prostatectomy (See letter of Support, GenomeDx).
    b. Evaluate high risk localized patients treated with or without neoadjuvant docetaxel and androgen deprivation therapy (NCT00430183).
    c. Evaluate pre-treatment metastatic biopsies from CRPC patients treated with abiraterone, and enzalutamide (IRB1305013903).
    d. Evaluate pre-treatment metastatic biopsies from NEPC patients treated with the Aurora A inhibitor MLN8237 (NCT01799278) on a Phase 2 clinical trial or the EZH2 inhibitor GSK126 (NCT02082977).

2. Specific Aim 2: Assess the impact of timing of N-Myc expression on the development of castration resistance and the NEPC phenotype.
    a. Assess the influence of N-Myc on the onset of CRPC and NEPC and associated molecular changes.

b. Assess the role of N-Myc/EZH2 complex for N-Myc dependent transcriptional regulation in establishing the NEPC phenotype.
c. Assess the role of N-Myc/Aurora-A complex for N-Myc dependent transcriptional regulation in establishing the NEPC phenotype

3. Specific Aim 3: Determine the impact of the timing of N-Myc on response to NEPC directed therapeutics.
   a. Monitor the impact of the timing of N-Myc expression in response to NEPC-related monotherapies *in vivo* and *in vitro.*
   b. Monitor the impact of the timing of N-Myc expression in response to NEPC-related combination therapies *in vivo* and *in vitro.*
   c. Mechanistic studies to determine NEPC-related molecular changes associated with EZH2 and Aurora A inhibition *in vitro* and *in vivo*

b. Accomplishments under these goals

1. Specific Aim 1: To assess the timing of N-Myc activation in patients and define how N-Myc signaling impacts response to aurora kinase A inhibition and clinical outcomes.

Clinical NEPC is associated with neural lineage.

Although there is a spectrum within the pathologic subtype of NEPC, we have found that NEPC tumor cells defined by morphologic features often lose AR expression and express neuroendocrine markers [1]. This observation suggests a transition from epithelial to neural lineage, which may involve dedifferentiation. To fully appreciate the spectrum of lineage states, we performed whole transcriptome analyses on patient samples, including the largest cohort of NEPC patients to-date. Gene expression was assessed from metastatic tumor biopsies of patients with pathology confirmed NEPC (n = 36) and CRPC-Adeno (n = 73), as well as from localized prostate adenocarcinoma (PCa) (n = 66). Relative to PCa, NEPC tumors demonstrated a significant enrichment for stem cell genes associated not only with normal neuroendocrine cell precursors (neural crest stem cells (NCSC)), but also with activated neural stem cells (aNSC) (**Figure 1A, Table S1**). Unsupervised clustering analysis of the NEPC versus PCa leading-edge genes from embryonic stem cells (ESC), NCSC or NSC genesets [2-4] segregated patients according to their tumor histological classification (PCa, CRPC-Adeno or NEPC, **Figure S1A**). Interestingly, the stratification of CRPC-Adeno and NEPC patients based on levels of *MYCN* expression correlated with expression of neural lineage genes and inversely with AR signaling (**Figure 1A, Figure S1B**). To further validate the association with NSC genes, we purified murine NSC from the sub-ventricular zone and performed RNA-seq and histone-3 lysine-4 tri-methylation (H3K4me3) chromatin immunoprecipitation followed by DNA sequencing (ChIP-seq). From these studies, we combined the upregulated genes marked by H3K4me3 with publicly available single-cell RNA-seq data from activated NSC [5] and revealed a similar enrichment of NSC pathways in NEPC patient samples versus PCa samples (**Figure 1A**).

Moreover, we observed that high *MYCN* expression in patient CRPC-Adeno tumors was significantly associated with a worse overall survival compared to those with low *MYCN* expression (37.7 versus 80.3 months, hazard ratio (HR) = 1.95, 95% confidence interval (CI) 0.92-4.09, p-value = 0.04). This was also true for patients with NEPC (25.9 versus 41.4 months, HR = 3.31, 95% CI 1.22-9.09, p-value = 0.0064) as well as the combined cohort of all 81 patients (34.0 versus 76.5 months, HR = 2.27, 95% CI 1.24-4.11, p-value = 0.002, **Figure 1B**). While these

data reveal that *MYCN* expression correlates with neural-lineage programs and poor clinical outcome, in both CRPC and NEPC patients, the underlying mechanism remains poorly described. We therefore sought to determine the precise mechanism that drives a prostate tumor epithelial cell to lose its luminal markers and gain a more neural-like lineage.

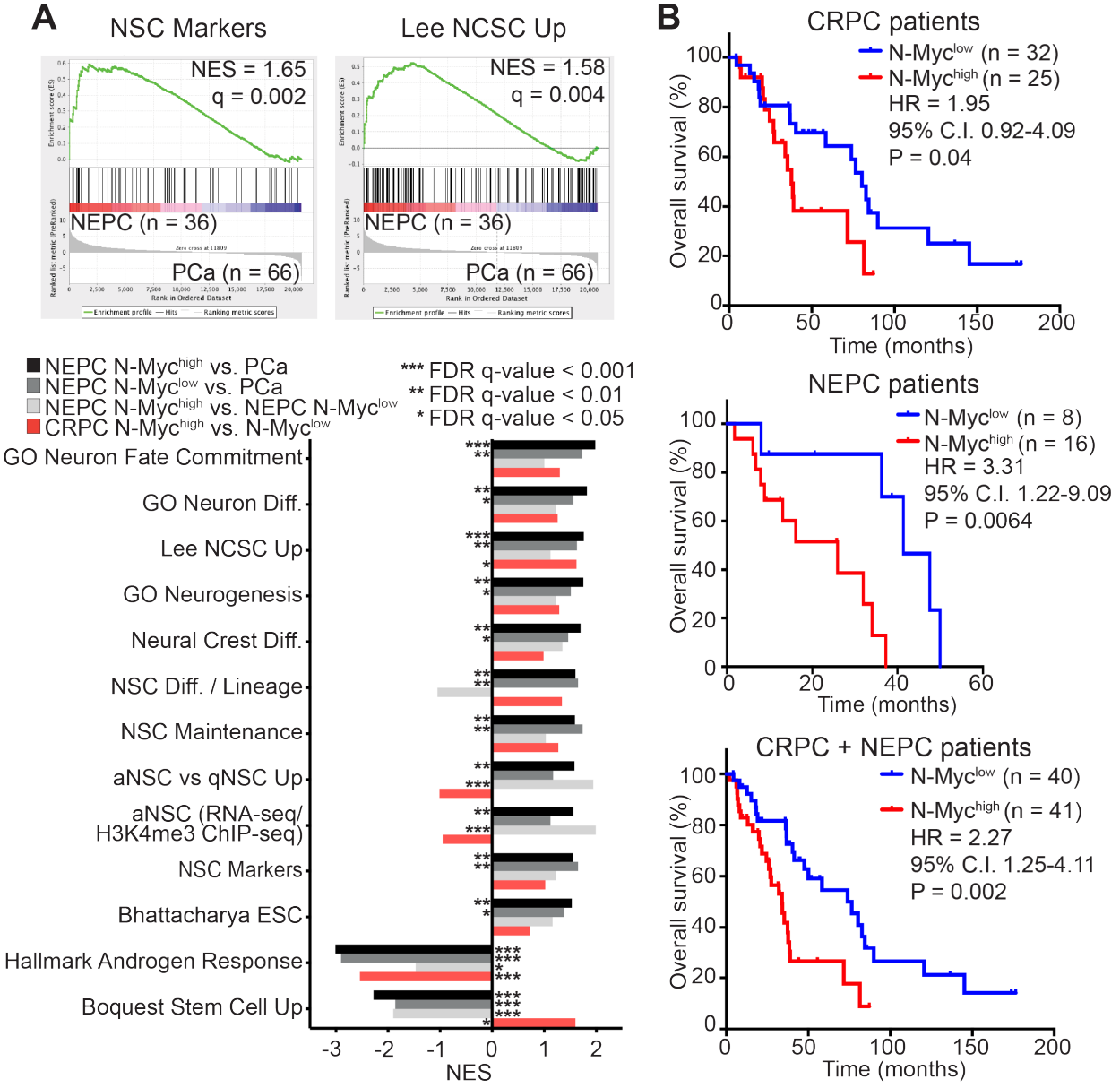

Figure 1. Clinical NEPC is associated with neural lineage. **(A)** Top: Enrichment plots of the Neural Stem Cell Markers and Lee Neural Crest Stem Cell Up genesets between indicated groups. Bottom: Targeted GSEA in the five NEPC samples with the highest (N-Myc^{high}) or lowest (N-Myc^{low}) level of *MYCN* expression versus PCa (n = 66) patient samples, NEPC N-Myc^{high} versus NEPC N-Myc^{low}, and on the five CRPC with the highest level of *MYCN* expression versus the five lowest. **(B)** Kaplan–Meier plots of CRPC (n = 57) patients, NEPC (n = 24) patients or CRPC+NEPC (n = 81) patients, stratified into two categories according to the median value of *MYCN* mRNA expression. Survival analysis was performed using the Kaplan-Meier estimator (log-rank test).

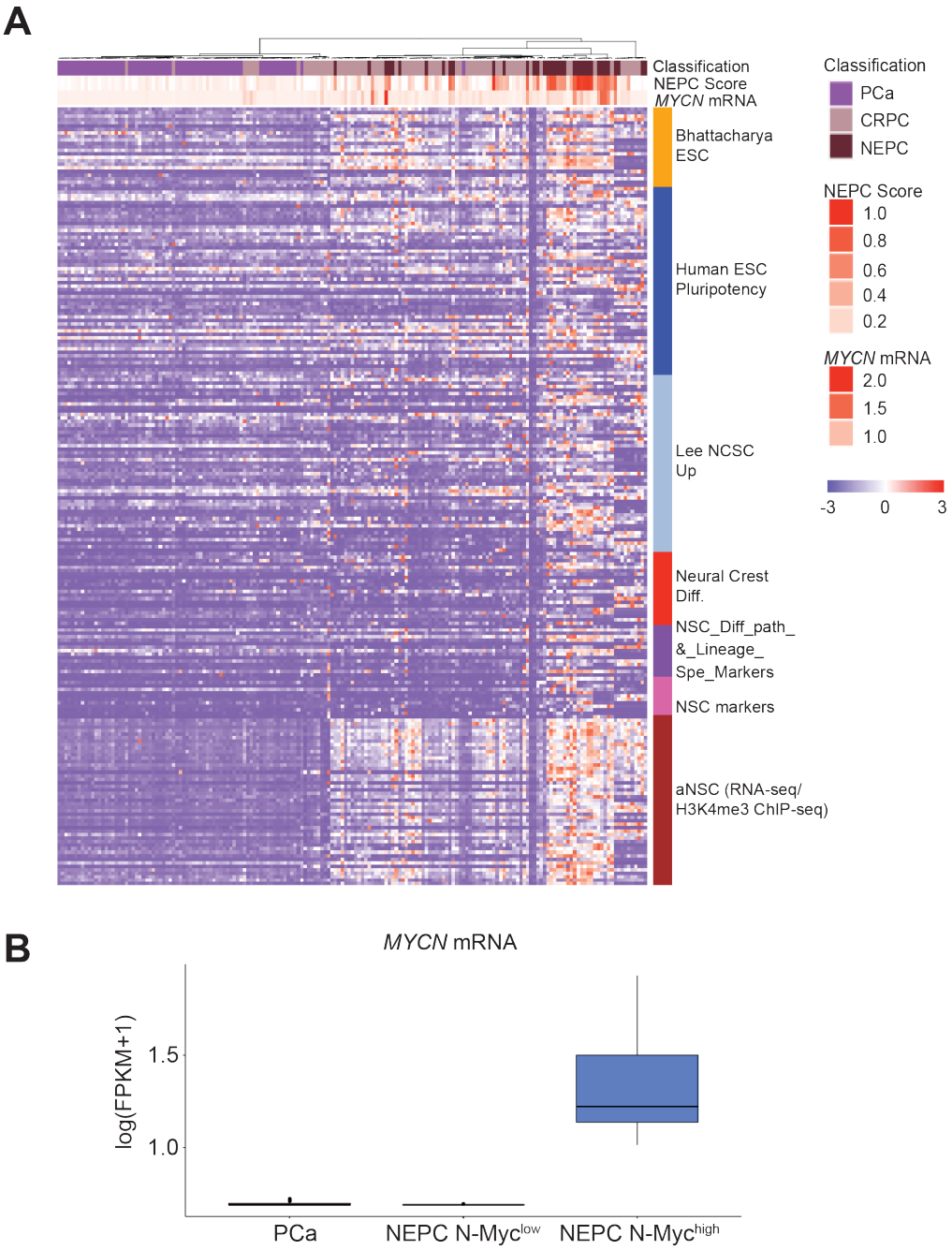

Figure S1. Clinical NEPC is associated with neural lineage. A) Clustering of PCa (n = 66), CRPC (n = 73) and NEPC (n = 36) patient samples classified based on the expression level of the leading edge genes of each geneset (NEPC versus PCa) indicated on the right. **B)** Expression of *MYCN* in PCa, NEPC N-Myc^{low} or NEPC N-Myc^{high} patients. Graph depicts the median value between the 25th and 75th percentiles with whiskers indicating the range within 1.5 IQR.

Table S1. Neuronal lineage and AR signaling-associated genesets.

Gene list	Human Embryonic Stem Cell Pluripotency	Bhattacharya_Embryonic _Stem_Cell	Ramalho_Stemness _Up	Boquest_Stem_Cell _Up	Lee_Neural_Crest _Stem_Cell_Up	Neural Crest Differentiation	Neural Stem Cell Differentiation Pathways and Lineage-specific Markers
From	Pathcards	GSEA Broad Institute	GSEA Broad Institute	GSEA Broad Institute	GSEA Broad Institute	Pathcards	Pathcards
Size	186	89	206	260	146	102	79

Gene List	Neural Stem Cell Markers	UP In Activated NSC Vs Quiescent NSC	UP In Quiescent NSC Vs Activated NSC	UP In NPC Vs Activated NSC	UP In Activated NSC Vs NPC	UP In Activated NSC Vs Quisecent NSC _ H3K4me3 And Expressed In Our Data aNSC	Hallmark_ Androgen_ Response
From	Rndsystems	PMID 28099854	PMID 28099854	PMID 28099854	PMID 28099854	PMID 28099854 Overlap With Our Data From aNSC	GSEA Broad Institute
Size	58	2287	606	357	385	1670	101

Gene list	Go_Neuron_ Differentiation	Go_Neuron_Fate_ Commitment	Go_ Neurogenesis	Go_Neural_ Crest_Cell_ Differentiation	Go_Stem_Cell_ Differentiation	Go_Neuronal_ Stem_Cell_ Population_ Maintenance	Smith signature ASC (only used for comparison with LNCaP cell data.)
From	GSEA Broad Institute	GSEA Broad Institute	GSEA Broad Institute	GSEA Broad Institute	GSEA Broad Institute	GSEA Broad Institute	PMID 30232014
Size	874	67	1402	75	190	19	50

N-Myc associated with response to alisertib (MLN8237). In a phase 2 trial of alisertib for patients with castration resistant and neuroendocrine prostate cancer (NCT01799278), 60 patients were treated. Median PSA was 1.1, number of prior therapies was 3, and approx. 70% of patients had visceral metastases. Although six month progression free survival was 13.5%, four exceptional responders were identified, including complete resolution of liver metastases, all of which had evidence of N-myc overactivity. Further analysis of metastatic pre-treatment biopsies and N-myc signatures genes is ongoing. Patient derived organoids of two patients on study (PM154, PM155) were developed that demonstrated concordant response in vitro as the patients did clinically and have been utilized for the dynamic testing of N-myc-Aurora complex formation and will be used for N-myc-EZH2 and other readouts.

N-Myc signaling in localized disease

In collaboration with GenomeDx, we analyzed transcriptome data of prostatectomy specimens from 9640 patients treated for localized prostate cancer with associated outcomes data. MYCN was expressed in approx 5% of localized prostate adenocarcinoma and did not associate with Gleason grade. MYCN expression correlated inversely with AR and positively with NEROG1, SOX11, AURKAIP1, and BRN2 expression. GSEA of this localized dataset also showed inverse correlation with EZH2 target genes, REST, and SUZ12 ($p<0.0001$; Pearson coeff >0.5). Further analysis, including neural genes, and correlation with clinical features and outcomes are ongoing.

2. Specific Aim 2: Assess the impact of timing of N-Myc expression on the development of castration resistance and the NEPC phenotype.

AR signaling alters the N-Myc transcriptome in vivo.

While N-Myc cooperates with Enhancer of Zeste Homolog 2 (EZH2) to abrogate AR signaling [6], the role of N-Myc in driving lineage plasticity in an NEPC-like context of low to no AR signaling has not been characterized. Using our previously described *Pb-Cre*$^{+/-}$*; Pten*$^{f/f}$*; LSL-MYCN*$^{+/+}$ genetically engineered mouse model (GEM) which overexpresses human *MYCN*, we found that N-Myc overexpression led to the formation of prostate tumors with 100% penetrance compared to *Pb-Cre*$^{+/-}$; *Pten*$^{f/f}$; *LSL-MYCN*$^{-/-}$ mice (**Figure S2A**). Interestingly, survival of *Pb-Cre*$^{+/-}$*; Pten*$^{f/f}$*; LSL-MYCN*$^{+/+}$ mice was increased by an average of 12 weeks in response to castration (**Figure S2A**). This is likely due to the fact that the tumors are heterogeneous with a component of AR-responsive adenocarcinoma, consistent with data from another GEM model of adenocarcinoma to NEPC transformation. Despite the prolonged survival, castrated mice developed invasive prostate tumors that metastasized to multiple locations, including the liver, at 6 months post-castration. We also noted an increase in poorly differentiated foci that lost expression of luminal (AR, cytokeratin 8 (KRT8)) and basal (KRT5) markers and gained expression of the epithelial-mesenchymal transition marker vimentin (VIM) and the NEPC marker neural cell adhesion molecule (NCAM1, **Figure 2A**). Primary and metastatic lesions in castrated mice contained tumor foci with up to 90% of the total tumor area comprised of divergent differentiation (e.g., intestinal, squamous, sarcomatoid as previously described or chondroid differentiation) compared to up to 25% in the intact animals (**Figure S2B,C**). In addition, we

observed large foci of neural differentiation characterized by ganglion-like cells. These cells had abundant eosinophilic cytoplasm and nuclei with prominent, centrally located nucleoli. Immunohistochemical staining of serial 4 µm tissue sections revealed populations of cells that were either positive for epithelial (AR and KRT8), mesenchymal (VIM) or neural markers (S100) but also contained cells that were positive for multiple lineages (AR and VIM) (**Figure S2D**). This suggests that these double positive cells may be transitioning from one lineage to another, similar to what has been observed in other mouse models. The ganglion differentiation is also consistent with previous observations made in N-Myc-driven neuroblastoma models. The loss of AR and gain of VIM and S100 suggest further differentiation towards the neural lineage, and some of the VIM/S100-positive cells have invaded the local vasculature (**Figure 2B**), consistent with a pro-metastatic phenotype. These data suggest that the removal of androgen signaling enables a wider variety of N-Myc-induced differentiation programs.

To further define the transcriptional differences regulated by N-Myc in an androgen-dependent manner, we performed RNA-seq on N-Myc-expressing 22Rv1 xenografts grown in castrated or intact recipients. Transcriptome-wide analyses revealed that castration was associated with a significant increase in the number of N-Myc-deregulated target genes (**Figure 2C)**. In castrated 22Rv1 xenograft mice, the N-Myc-signature was enriched with genes associated with neural lineage pathways (**Figure 2C**), including neural progenitor cells (NPC) bivalent genes (H3K4me2/3 active and H3K27me3 repressive marks [7,8], NES = 2.00, FDR q-value = 0.004), in addition to genes implicated in neural development (e.g. *SOX11, SOX21, NTRK1, NKX2-1*), expressed in adult stem cells (e.g. *HOXA2/A3/A9/A10* and *WNT5A*), ES cells (e.g. *SOX2*) or NEPC (e.g. *CHGA*), while epithelial–lineage associated genes were downregulated (**Figure 2C**). Similar observations were made in the GEM model (**Figure S2E**). Importantly, both 22Rv1-CTL and 22Rv1-N-Myc cells express the AR variant ARv7 (**Figure S3A/B**). Despite ARv7 expression, androgen response genesets were significantly downregulated in response to castration, as observed by gene set enrichment analysis (GSEA) (**Figure S3C**), and N-Myc expression blocked the upregulation of ARv7 target genes after castration (**Figure S3D**). These data suggest that the removal of circulating androgen and AR signaling may impact N-Myc gene regulation. Since these datasets were generated from tumors following chronic androgen deprivation, we cannot rule out that these molecular changes did not evolve over time.

N-Myc expression leads to neural lineage gene expression and reduced androgen response.

To directly assess the impact of acute removal of androgen on the N-Myc-induced molecular program, we performed, in replicate, RNA-seq in isogenic LNCaP cells (+/- *MYCN* [6]) following short-term androgen withdrawal. LNCaP cells, a hormone-naive prostate cancer cell line with a well-characterized luminal/epithelial phenotype, were starved in androgen-deprived media for 72 hours, and subsequently re-exposed to androgen or maintained in androgen-deprived conditions for an additional 24 hours (**Figure 3A**). RNA-seq data revealed a distinct N-Myc driven transcriptional program with 8,585 genes differentially regulated in N-Myc cells compared to control (CTL) cells (**Figure S4A**). Consistent with our observations in vivo, androgen withdrawal significantly altered the N-Myc signature in vitro (13% and 42% of the N-Myc target genes are differentially regulated specifically in the presence or absence of androgen, respectively, **Figure S4A**). While, in the presence of androgen, AR signaling was enriched in LNCaP-CTL cells compared to N-Myc cells as expected [6] (**Figure 3B**), N-Myc-upregulated genes were enriched with stem cell signatures and markers of neural lineage differentiation in the absence of androgen (**Figure 3B**). These changes were shown to be N-Myc-dependent, as shRNA-mediated knockdown of N-Myc reversed their expression (e.g. *AUTS2* and *NKX2-1*, **Figure S4B**). To determine if the transcriptional changes were stable, we maintained cells in androgen-deprived condition for 41 days followed by a 24-hour androgen stimulation (**Figure 3A**). After long-term

withdrawal, the response of AR-target genes to androgen stimulation was dramatically reduced (over 80% for *KLK4*, **Figure 3C**). Moreover, expression of genes associated with the neural lineage were increased significantly in LNCaP-N-Myc cells (**Figure 3C,D, Figure S4C,D**) and N-Myc expression led to increased enrichment at day 42 compared to day 4 for neural lineage and stem cell genesets, including an adult stem cell signature associated with small cell neuroendocrine cancers from multiple epithelial tissues. N-Myc expression was also associated with reduced global responsiveness to androgen re-stimulation, with fewer genes being differentially expressed at day 42 in LNCaP-N-Myc cells compared to LNCaP-CTL cells (**Figure 3E**). Altogether, these data support the hypothesis that there is interplay between AR and N-Myc signaling that propagates lineage plasticity.

The N-Myc cistrome is distinct from C-Myc and altered by AR signaling.

As a transcription factor, N-Myc regulates gene expression by binding to DNA and modulating transcriptional activity. To fully describe the genomic loci where N-Myc is bound, we performed N-Myc ChIP-seq in LNCaP-N-Myc cells or isogenic LNCaP-CTL cells following acute androgen withdrawal (**Figure 3A**). We observed N-Myc binding as a narrow peak mainly within 2 kilobases (Kb) of gene transcription start sites (TSS, **Figure 4A**) irrespective of androgen. Approximately 40%, 25% and 25% of N-Myc peaks were within intronic, intergenic and promoter/TSS regions, respectively. To define N-Myc-specific binding in prostate cancer cells, we compared the N-Myc cistrome (LNCaP-N-Myc cells with androgen) with the C-Myc cistrome (LNCaP cells with androgen) and with publicly available N-Myc ChIP-seq data from a *MYCN*-amplified neuroblastoma model. Approximately half of the N-Myc bound sites were shared with C-Myc in LNCaP cells and/or N-Myc in neuroblastoma cells (**Figure 4B,C**). The genes uniquely bound by C-Myc in LNCaP cells were enriched with cell cycle and cell proliferation-related genes, corresponding to the most well characterized functions of Myc family proteins, while the genes uniquely bound by N-Myc in neuroblastoma cells were neural lineage-related. Despite these overlaps, we observed that 44% of the N-Myc bound sites are specific to the prostate cancer cells and that these prostate-specific N-Myc-bound genes are enriched for neural-lineage genes (**Figure 4D**). Moreover, while the C-Myc-specific and N-Myc/C-Myc-shared bound sites were enriched for E-box motifs, the N-Myc-specific sites in LNCaP cells were significantly enriched for Forkhead motifs (**Figure S5A**). The difference between N-Myc and C-Myc binding in prostate cancer cells is also in accordance with the different profiles of expression of *MYC* and *MYCN* mRNA in prostate adenocarcinoma (high *MYC*, low *MYCN*) versus NEPC (low *MYC*, high *MYCN*, **Figure S5B**). Intriguingly, N-Myc binds near the TSS of the *MYC* locus and may help to enforce the selective pattern of N-Myc/C-Myc expression (**Figure S5C**). Together these results suggest that, while Myc-family members share a number of common targets, they are not completely functionally-redundant and have specific targets, that are regulated in a cell type-dependent manner.

To determine if the androgen-dependent changes in gene regulation were explained by a change in N-Myc binding to chromatin, we compared the binding profiles obtained in the two conditions. We found that 42% of N-Myc binding was dynamic, changing in different contexts of AR signaling (**Figure 4E**). Upon androgen withdrawal, N-Myc binding was depleted or reduced from 36% of total bound sites, while enriched or newly bound to 6% (**Figure 4E, Figure S5D**). These dynamic N-Myc peaks were less enriched at promoter/TSS regions and more enriched at intergenic and intronic regions (**Figure 4E)**. The distribution of dynamic N-Myc binding was confirmed by performing ChIP-seq in N-Myc-expressing 22Rv1 xenografts from castrated or intact recipients (**Figure 4E**). We also found that the peaks shared with and without androgen were closer to TSS than the peaks specific to one condition (**Figure S5E**) and were enriched at genes involved in normal cellular homeostasis (**Figure S5F**).

N-Myc interacts with known AR co-factors to alter DNA binding.

Differential interactions between N-Myc and transcriptional co-factors or pioneering factors could explain the observed dynamic binding genome-wide. It has been shown that less than half of Myc binding sites on chromatin have consensus E-box motifs and many do not even show variant E-boxes, concluding that the E-box enhances chromatin association but is not a prerequisite for binding. Most likely, therefore, protein/protein interactions play a large role in targeting N-Myc to sites on chromatin. To reveal such co-factors, we performed a de novo motif discovery in 200 bp regions surrounding all N-Myc binding sites identified by ChIP-seq. Motif analysis of the unique and enriched N-Myc peaks revealed that, in addition to E-boxes, there was a significant enrichment of motifs consistent with forkhead box (FOX) and homeobox (HOX) family members (**Figure 5A, Figure S6A**). Since FOXA1 and HOXB13 are critical AR-coregulators, we performed HOXB13 and FOXA1 ChIP-seq in the LNCaP-N-Myc cells. Unlike for HOXB13, we found that androgen withdrawal dramatically altered the FOXA1 cistrome (31% unique peaks, **Figure 5B**). With respect to the unique N-Myc peaks in the absence of androgen, there was very little overlap (< 20%) with the C-Myc, N-Myc in neuroblastoma or AR cistromes, compared to the N-Myc common peaks (**Figure 5C**). In contrast, N-Myc unique peaks without androgen shared more binding sites with AR co-factor cistromes defined in the presence of androgen in N-Myc cells versus CTL cells (from 39% to 51% for FOXA1 and from 12% to 29% for HOXB13). This overlap was further increased for FOXA1 following androgen withdrawal (+10%, **Figure 5C**). Taken all together, 57% of all enriched and unique N-Myc peaks without androgen were co-bound with AR, HOXB13 or FOXA1 either alone or in combination (**Figure 5D**). In agreement with the motif analysis, comparison of the genomic loci bound by N-Myc after androgen withdrawal revealed nearby binding of FOXA1 and/or HOXB13 (**Figure 5E).** Furthermore, while epithelial lineage genes were enriched at these co-bound sites as expected, there was also a significant enrichment of neural lineage genesets (**Figure S6B**). To directly assess the ability of a prostate lineage-defining factor, such as FOXA1, to modulate N-Myc binding at neural lineage genes, we performed siRNA-mediated knockdown of FOXA1 and performed N-Myc ChIP-qPCR at binding sites identified by ChIP-seq (**Figure 5F**). Despite a knockdown of only 50%, we observed a significant decrease in N-Myc binding on the target neural genes *NKX2-1* and *CHGA*, suggesting a role for FOXA1 in regulating N-Myc binding (**Figure 5F**).

To identify other proteins that could regulate N-Myc binding, we performed Rapid Immunoprecipitation Mass Spectrometry of Endogenous Proteins (RIME) [9] in LNCaP-N-Myc cells. While a subset of common interactors demonstrated increased affinity between the conditions, no interactions specific to one condition versus another were observed (**Figure 5G**). The majority of interactions were shared between conditions and included well-known N-Myc interacting proteins (e.g. MAX and TRRAP), proteins associated with heterochromatin (e.g. chromobox homologs (CBX) 1, 3 and 5) as well as HOXB13 (**Figure 5G**). These data suggest that, while the ability to physically interact with N-Myc is not dramatically affected by the presence or acute withdrawal of androgen, N-Myc co-factors may direct genomic binding to sites in chromatin that are accessible specifically in one condition either through competition at N-Myc binding sites or by altering the chromatin accessibility.

N-Myc promotes bivalency on neural lineage genes.

On a global scale, gene transcription is also regulated by epigenetic modifications of histone proteins. Two of the major histone marks used to study the regulation of gene expression are H3K4me3 (associated with transcriptional activation) and H3K27me3 (associated with repression). Paradoxically, some genomic loci contain both marks (i.e. bivalent). Bivalently marked genes are typically transcriptionally poised, have been well characterized in ES cells and shown to be essential for development and lineage-determination. The bivalent mark changes during the differentiation of the cells, through the action of histone modifiers, and biases gene expression towards activation (H3K4me3 only) or repression (H3K27me3 only) depending on

the identity of each cell. To interrogate a putative role of N-Myc in regulating bivalency, we assessed the overlap between H3K4me3 and H3K27me3 ChIP-seq profiles, following short-term or long-term androgen withdrawal (**Figure 3A**). Interestingly, the distribution and density of H3K27me3 histone marks near H3K4me3 marks varied dramatically depending on N-Myc expression and androgen stimulation. While the H3K27me3 binding profile was narrow and centered on H3K4me3 peaks in LNCaP-CTL cells, the binding was redirected within a 3 Kb range around the H3K4me3 peaks in LNCaP-N-Myc cells yielding a multimodal distribution (**Figure 6A**). We also observed similar numbers of genomic loci marked by H3K4me3 alone, while only N-Myc-overexpressing cells showed a significant increase in H3K27me3 (8.6-fold) and bivalent peaks (18-fold, **Figure 6B**) after androgen withdrawal. Bivalent genes in N-Myc cells were enriched for Polycomb Repressor Complex 2 (PRC2), neurogenesis and neural lineage pathways while bivalent genes in control cells were associated with gene regulation and stress response (**Figure 6B).** Integrating the RNA-seq data with H3K4me3/H3K27me3 ChIP-seq data revealed, as expected, low levels of gene expression associated with bivalent histone marks (**Figure S7A**). Interestingly, we found an increase of nearly 2-fold in the number of N-Myc peaks that are bivalent in absence versus presence of androgen, corresponding to 966 and 580 genes respectively (**Figure 6C, Table S3**). Moreover, androgen withdrawal dramatically increased the level of enrichment of PRC2 and neural-associated genes (**Figure S7B**). Among the N-Myc-bound, bivalent genes, a subset showed a decrease of H3K4me3 and an increase of H3K27me3 levels in the absence of androgen. An example of this was observed for the desmocollin 3 gene (*DSC3)*, which has been implicated in epithelial cell junctions. Inversely, many genes associated with the neural lineage, such as *NKX2-1, SOX2, SOX11* and *SOX21*, became bivalent by gaining H3K4me3 marks in the N-Myc cells, suggesting the activation of gene expression (**Figure 6D, Figure S7C**). Binding at these regulated loci appeared to be specific for N-Myc in LNCaP cells compared to C-Myc in LNCaP and/or N-Myc in neuroblastoma (**Figure S7D**). Similar results were obtained by performing N-Myc/H3K4me3/H3K27me3 ChIP-seq in a NEPC patient-derived organoid (PM154, **Figure 6D, Figure S7C**). We thus hypothesized that the bivalent genes linked to neuronal identity would maintain H3K4me3 and be up-regulated following chronic androgen withdrawal, while the genes associated with an epithelial lineage would maintain H3K27me3 and become down-regulated over time. To assess this, we analyzed the expression levels of the 966 bivalently-marked, N-Myc-bound genes by RNA-seq following acute or chronic androgen withdrawal. Genes that were identified as bivalently-marked and N-Myc-bound at day 4, were enriched in LNCaP-N-Myc versus LNCaP-CTL cells, at day 42 (**Figure 6E**). Unsupervised clustering of the differentially expressed genes in LNCaP N-Myc versus LNCaP-CTL cells at day 42 revealed distinct transcriptional modules (**Figure 6F**). Cluster 1 included repressed epithelial-related or AR target genes (*ZBTB7A, ALDH1A3*), consistent with an increase of the repressive mark H3K27me3 on AR target genes (**Figure S4D**) and with previous findings [6]. Conversely, Cluster 4 contained many of the neural lineage genes, which are upregulated by N-Myc following long-term androgen withdrawal (**Figure 6F**). Furthermore, we confirmed that 57% of the 966 bivalently-marked, N-Myc-bound genes at day 4 became marked only with H3K4me3 at day 42, with 30% remaining bivalently marked (**Figure S8A,B**), and the genes which became H3K4me3 marked only were significantly enriched for neural lineage genesets (**Figure S8C**).

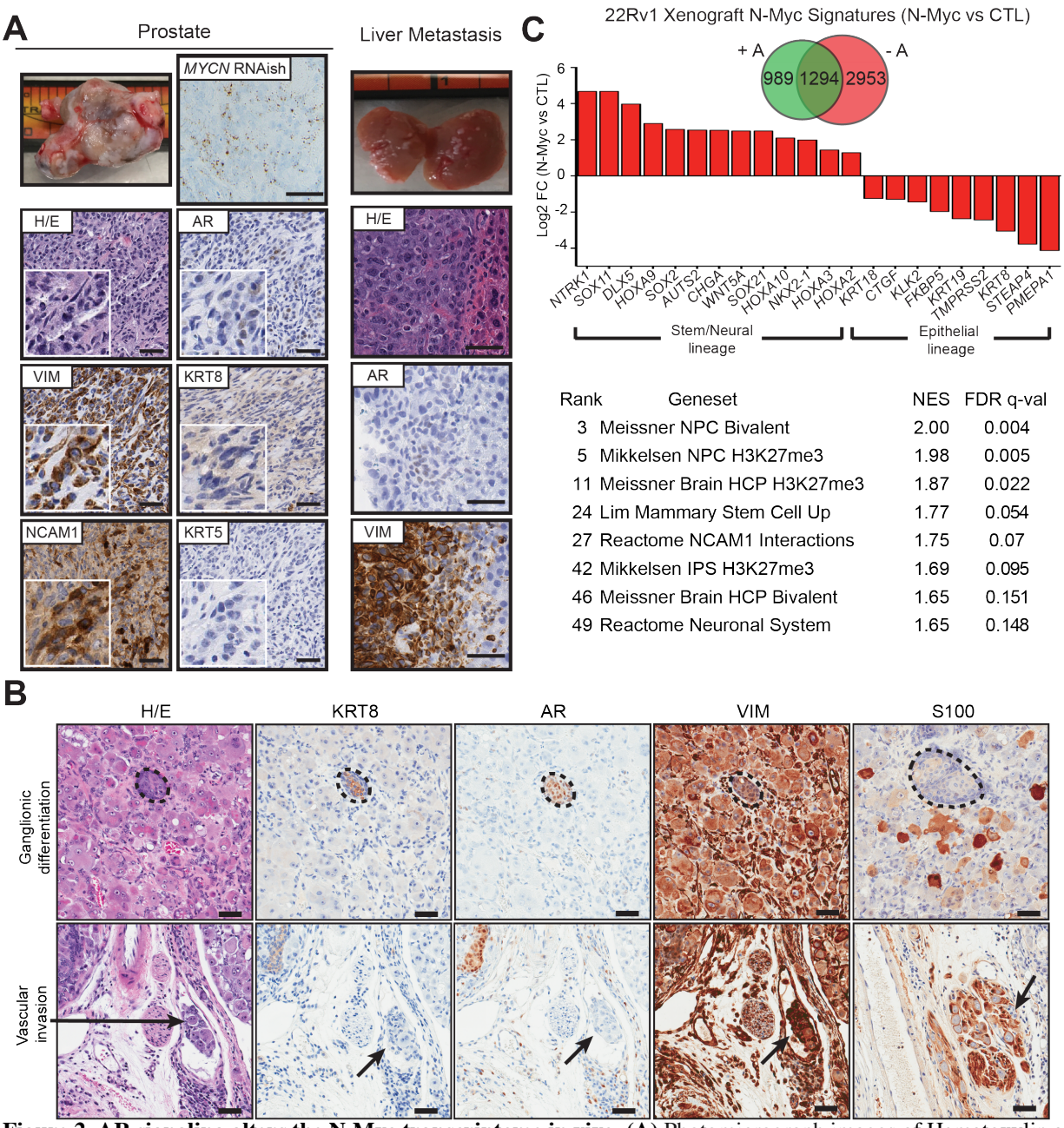

Figure 2. AR signaling alters the N-Myc transcriptome in vivo. (A) Photomicrograph images of Hematoxylin and Eosin (H/E) staining, vimentin (VIM), NCAM1, AR, cytokeratin 8 (KRT8) and 5 (KRT5) immunohistochemistry on primary prostate tumor region enriched with sarcomatoid differentiation (left) or liver metastatic lesion (right) from *Pb-Cre*$^{+/-}$*; Pten*$^{f/f}$*; LSL-MYCN*$^{+/+}$ mice 6 months after castration (scale bar = 50 μm). **(B)** Photomicrograph images of H/E staining or IHC staining for epithelial markers (AR and KRT8), a mesenchymal (vimentin (VIM)) or neural/ganglionic marker (S100) on 4μm serial sections from mouse C1 **(Fig. S2)**. Dotted lines indicate conventional adenocarcinoma adjacent to neural/ganglionic cells. Arrows indicate VIM/S100 positive tumor cells that have invaded local vasculature. (scale bar = 50μm) **(C)** Top: N-Myc signatures defined from 22Rv1-N-Myc xenografts versus 22Rv1 control (CTL) xenografts (-1 < log2(fold change) < 1, adj. p-value < 0.05, n = 3 biological replicates per condition). Bottom: GSEA analysis results comparing N-Myc castrated tumors versus the other 3 groups of tumors.

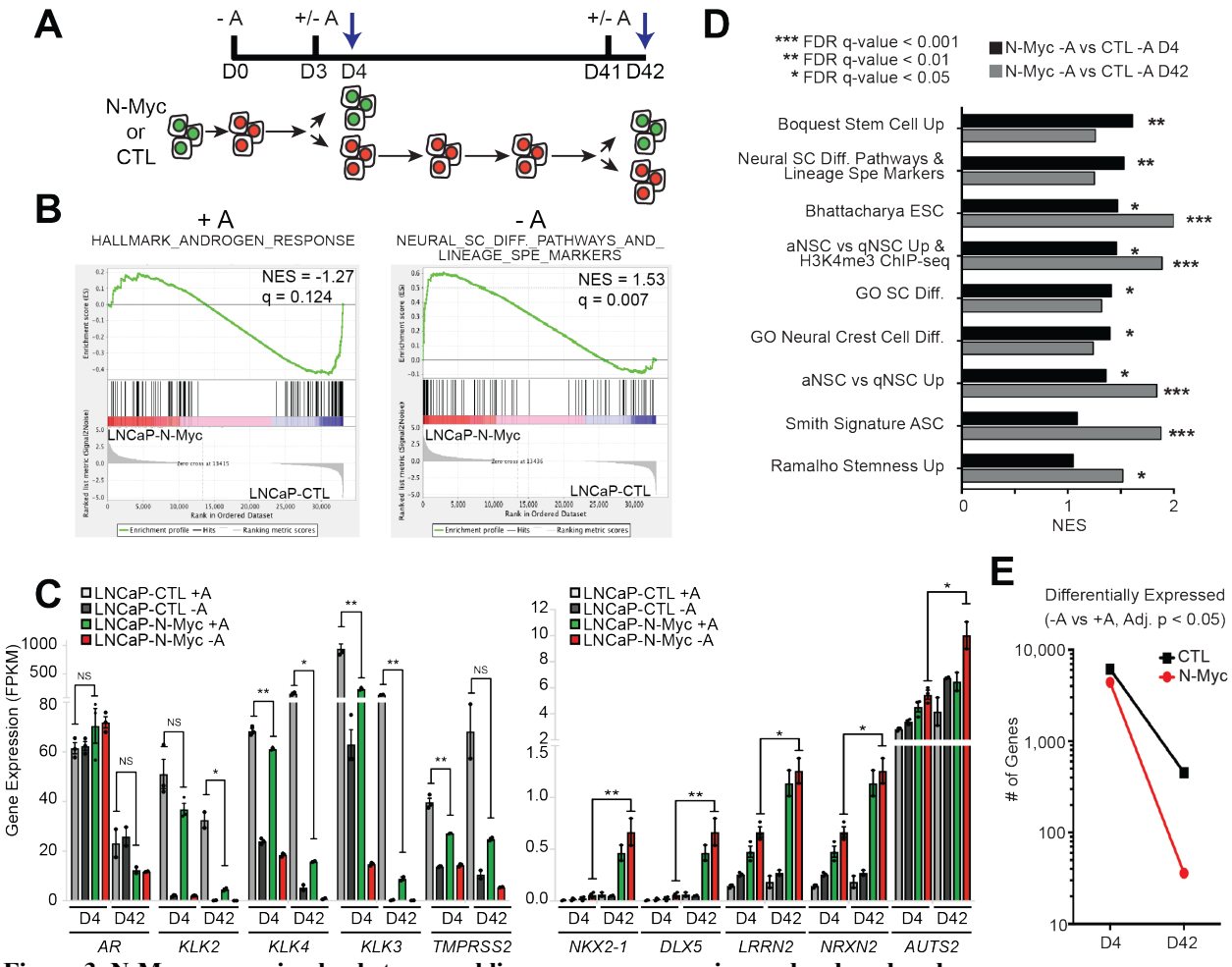

Figure 3. N-Myc expression leads to neural lineage gene expression and reduced androgen response.
(A) Experimental schematic with LNCaP-N-Myc or CTL cells and corresponding time points for RNA-seq or ChIP-seq analyses (arrows) in the presence (+A, green) or absence (-A, red) of androgen. **(B)** Enrichment plots for the Androgen Response and the Neural Stem Cell Differentiation Pathways and Lineage-specific Markers genesets from indicated conditions. **(C)** Gene expression (FPKM) of AR target genes (left) and neural lineage-associated genes (right) measured by RNA-seq in the indicated cells and conditions, at day 4 (D4, n = 3 biological replicates) and day 42 (D42, n = 2 biological replicates) of androgen withdrawal. * $p < 0.05$, ** $p < 0.01$, Student's unpaired two-tailed t-test. **(D)** Targeted GSEA on RNA-seq data from LNCaP-N-Myc versus CTL cells, without androgen, at D4 or D42 as indicated. **(E)** Number of genes differentially expressed (adj. p-value < 0.05) in the indicated conditions.

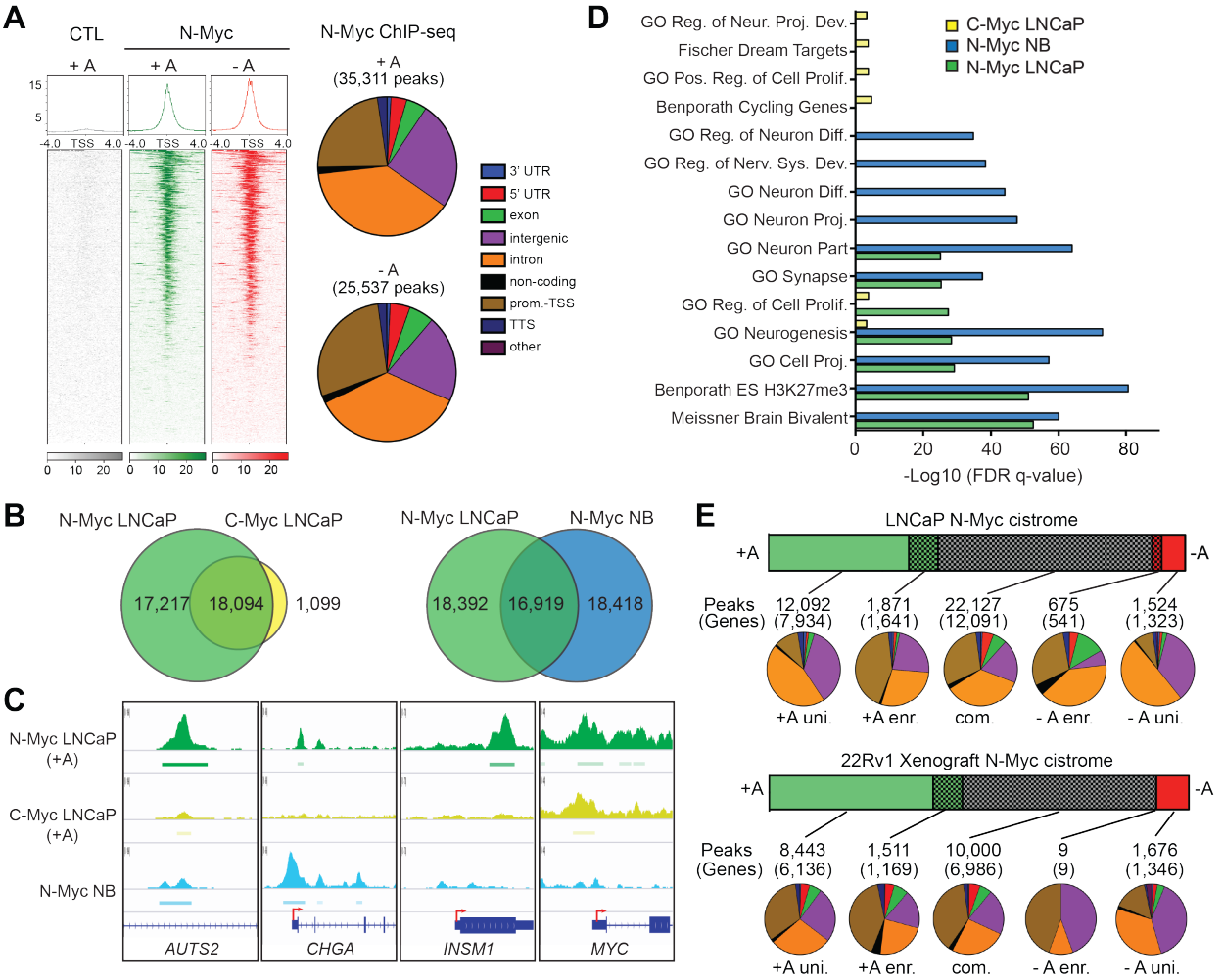

Figure 4. The N-Myc cistrome is distinct from C-Myc and is altered by androgen signaling.
(A) Left: Distributions and heatmaps of N-Myc ChIP-seq data generated from cells at day 4 (D4). Right: Proportion of N-Myc-bound sites at the indicated genomic annotation. **(B)** Overlap of Myc family member binding in prostate cancer cells (LNCaP, left) or N-Myc in prostate cancer cells versus published N-Myc in neuroblastoma cells (LNCaP/BE2C, right). **(C)** Examples of ChIP-seq tracks for indicated genes. **(D)** GSEA performed on the uniquely bound genes as identified in **(B)**. **(E)** Representation of N-Myc binding sites determined by ChIP-seq in LNCaP-N-Myc cells with and without androgen (top) or in 22Rv1 xenografts grown in castrated or intact recipients (bottom), and their distribution throughout the genome (n = 2 biological replicates per condition).

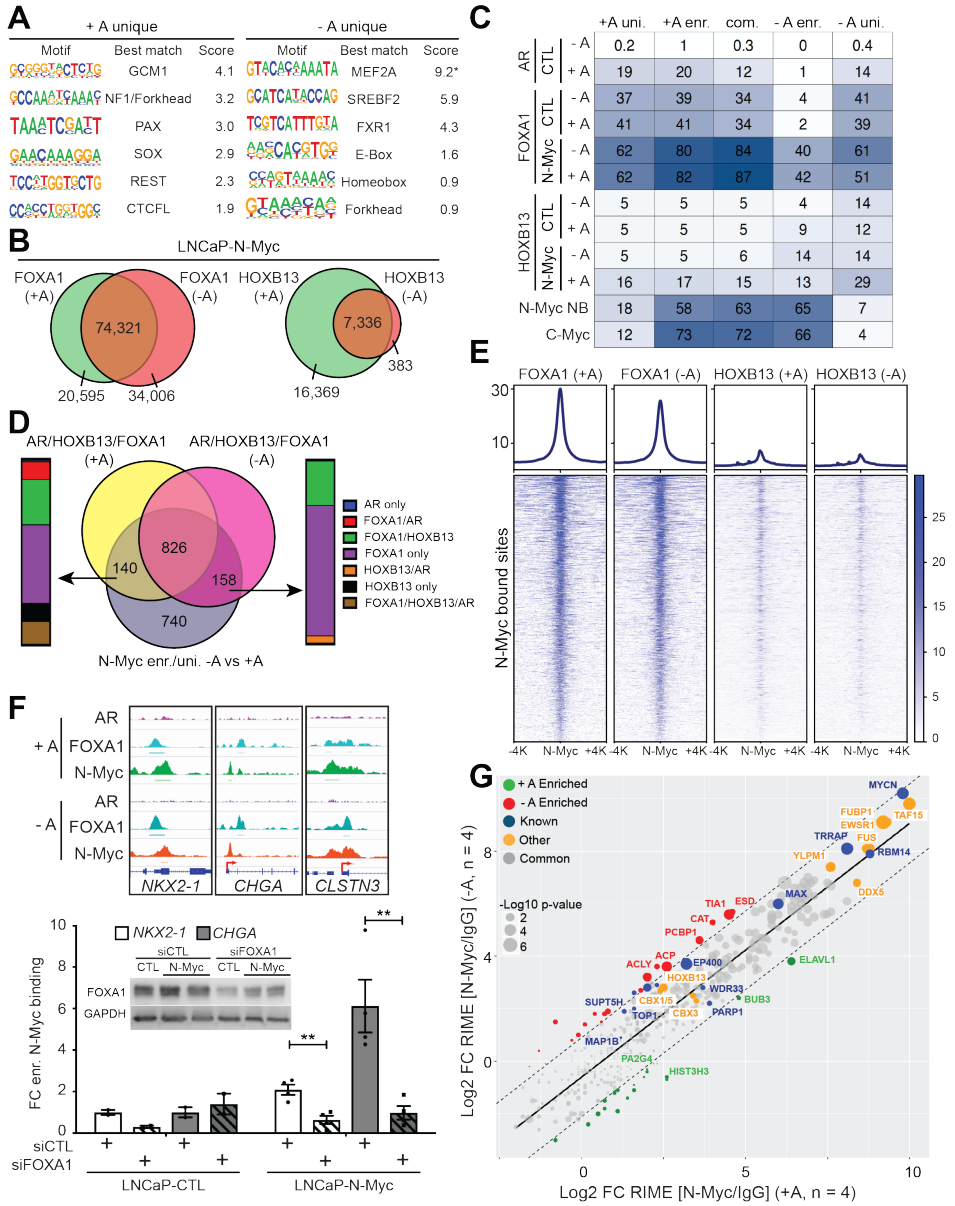

Figure 5. N-Myc interacts with known AR co-factors to alter DNA binding.

(A) Motif analysis of unique N-Myc peaks with or without androgen obtained by ChIP-seq in LNCaP-N-Myc cells. Scores correspond to log2 (% target / % background). All motifs shown are enriched with a p-value < 10^{-5} and are listed with their best predicted match to a known protein family. * % background of MEF2A motif was 0% and was subsequently adjusted to 0.001% to calculate a score. **(B)** Overlap between FOXA1 or HOXB13 ChIP-seq peaks in the LNCaP-N-Myc cells in the presence or absence of androgen at day 4. **(C)** Comparison of N-Myc binding with AR (GSE69045), FOXA1 (CTL cells: GSE69045) and HOXB13 binding with or without androgen, N-Myc in BE2C neuroblastoma cells (GSE80151) and C-Myc in LNCaP. Numbers represent the percentage of N-Myc peaks in each condition overlapping with the indicated co-factor. **(D)** Overlap of N-Myc peaks (enriched and unique in -A) with AR, HOXB13 or FOXA1 peaks in the indicated conditions. **(E)** Distribution of FOXA1 and HOXB13 binding at N-Myc bound sites +/- 4Kb in the indicated conditions. **(F)** Top: ChIP-seq tracks of genes co-bound by N-Myc and FOXA1, independently of AR (in CTL cells), in the indicated conditions. Bottom: Effect of FOXA1 knockdown by siRNA (see Western blot inset) on N-Myc binding assessed by ChIP-qPCR. ** $p < 0.01$, Student's unpaired two-tailed t-test. **(G)** Scatter plot of log2(fold change of N-Myc bound peptides versus IgG-bound peptides, identified by RIME) with (X-axis) and without (Y-axis) androgen (n = 4 biological replicates per condition). Lines correspond to the regression line +/- 1.7 Z.

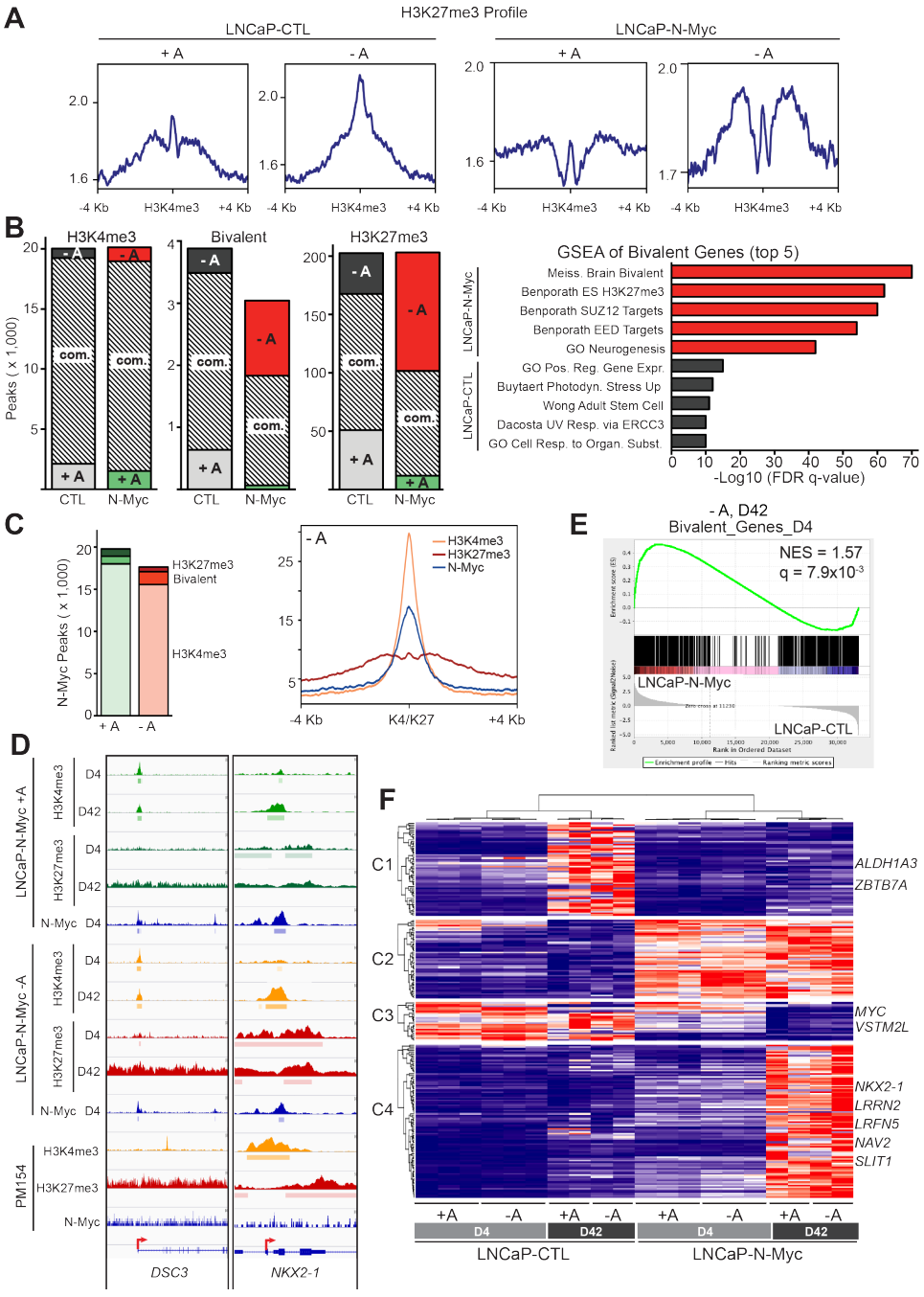

Figure 6. N-Myc promotes bivalency on neural lineage genes.
(A) H3K27me3 binding profiles within 8Kb centered at H3K4me3 peaks in LNCaP CTL and N-Myc cells, with and without androgen as specified. **(B)** Left: number of H3K4me3, H3K27me3 or H3K4me3/H3K27me3 bivalent peaks in common or unique to the conditions at D4 as indicated. Right: top 5 genesets from GSEA for uniquely bivalently marked genes in the absence of androgen from LNCaP-N-Myc cells (red) or CTL cells (black). **(C)** Left: Number of H3K4me3, H3K27me3 and bivalent peaks also bound by N-Myc with or without androgen. Right: H3K4me3, H3K27me3 and N-Myc binding profiles on bivalent peaks within 8Kb centered at H3K4me3 peaks, in LNCaP-N-Myc cells in the absence of androgen. **(D)** Examples of N-Myc and histone mark ChIP-seq tracks as indicated. **(E)** Enrichment plot of the bivalent genes identified in LNCaP-N-Myc -A cells at D4 measured in LNCaP-N-Myc -A cells vs LNCaP-CTL -A cells at D42. **(F)** Unsupervised clustering of the genes that were bivalent at D4 and differentially expressed (adj. $p < 0.05$) between LNCaP-N-Myc and LNCaP-CTL cells without androgen at D42.

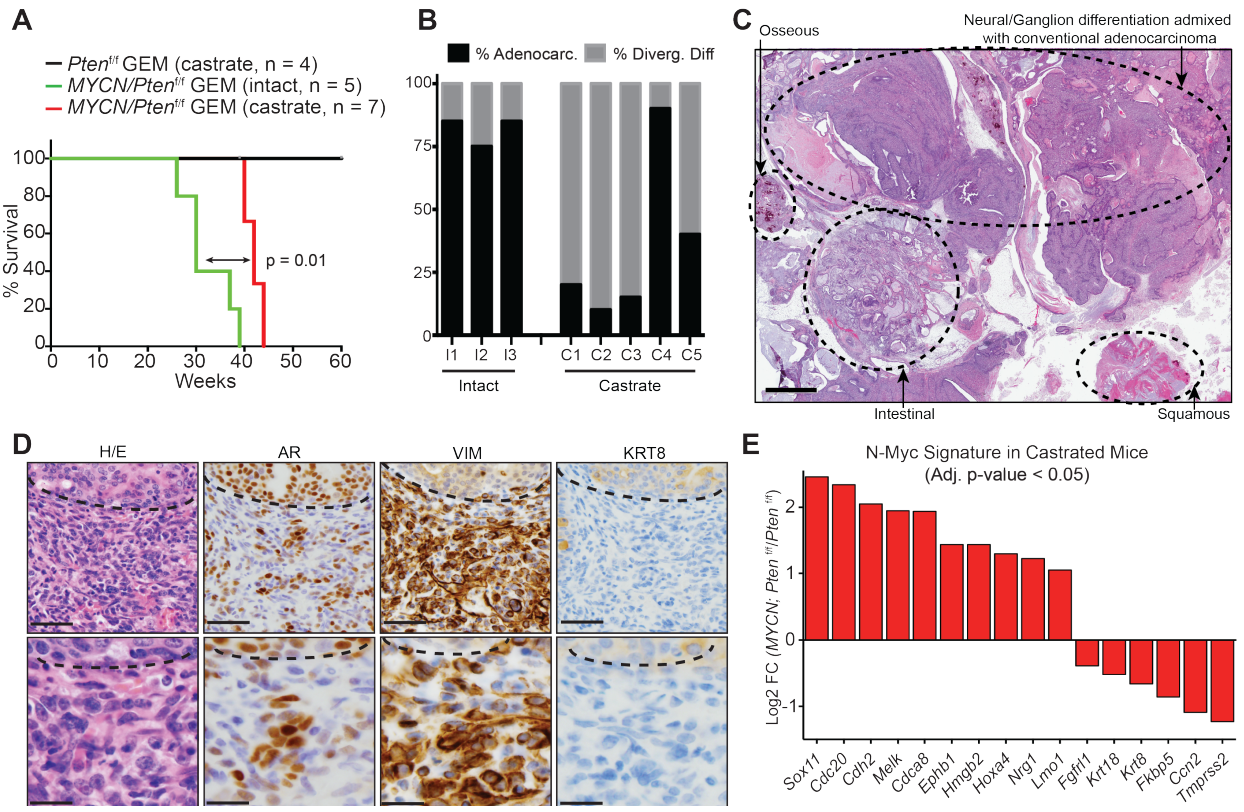

Figure S2. N-Myc promotes the acquisition of alternative lineage states in response to castration.
(A) Survival curve of castrated or intact GEM as indicated. Survival analysis was performed using the Kaplan-Meier estimator (log-rank test). **(B)** Percentage of tumor foci with adenocarcinoma or divergent differentiated tumor tissue in 10-12 month old intact or castrated *Pb-Cre*$^{+/-}$; *Pten*$^{f/f}$; *LSL-MYCN*$^{+/+}$ mice based on pathologist assessment. **(C)** Low power photomicrograph of a representative H&E-stained section from mouse C1 **(B)** showing the diversity of indicated histologies (dotted lines) (scale bar = 3mm). **(D)** Higher magnification (scale bar = 50µm) photomicrograph images of H/E staining or IHC staining for epithelial (AR and KRT8) or mesenchymal (VIM) marker on 4µm serial sections from mouse C5 **(B)**. Dotted lines indicate conventional adenocarcinoma adjacent to mixed lineage cells. **(E)** Examples of deregulated genes in *Pb-Cre*$^{+/-}$*; Pten*$^{f/f}$*; LSL-MYCN*$^{+/+}$ mice versus *Pten*$^{f/f}$ mice following castration (n = 3 biological replicates per condition).

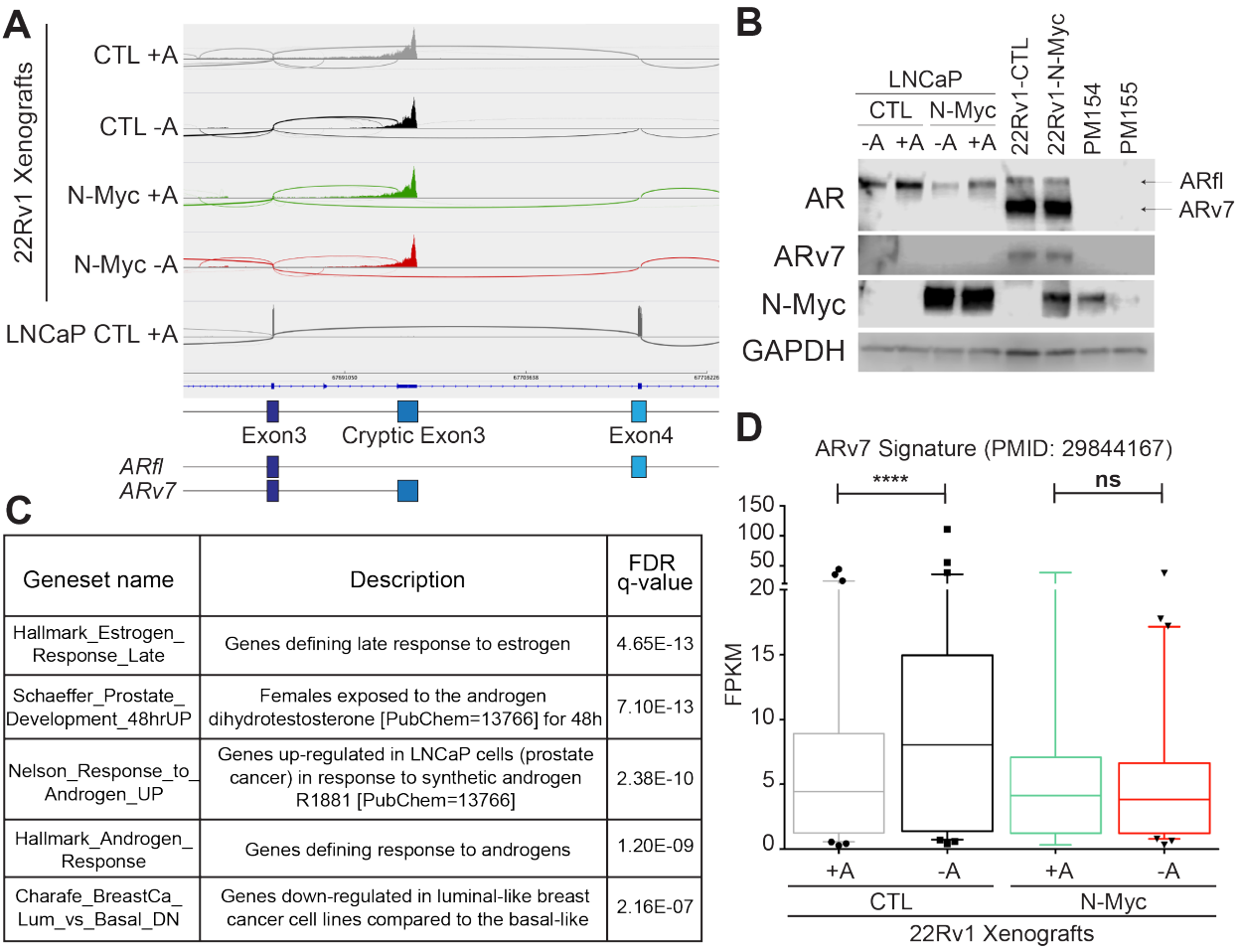

C

Geneset name	Description	FDR q-value
Hallmark_Estrogen_ Response_Late	Genes defining late response to estrogen	4.65E-13
Schaeffer_Prostate_ Development_48hrUP	Females exposed to the androgen dihydrotestosterone [PubChem=13766] for 48h	7.10E-13
Nelson_Response_to_ Androgen_UP	Genes up-regulated in LNCaP cells (prostate cancer) in response to synthetic androgen R1881 [PubChem=13766]	2.38E-10
Hallmark_Androgen_ Response	Genes defining response to androgens	1.20E-09
Charafe_BreastCa_ Lum_vs_Basal_DN	Genes down-regulated in luminal-like breast cancer cell lines compared to the basal-like	2.16E-07

Figure S3. Expression of ARv7 signatures are downregulated by N-Myc.
(A) Splicing map of *AR* RNA-seq transcripts from 22Rv1-CTL and 22Rv1-N-Myc xenografts grown in intact (+A) or castrated (-A) recipients showing splicing and inclusion of cryptic exon 3 (encoding ARv7). LNCaP cells depicted as a negative control. **(B)** Western blot for AR, ARv7 and N-Myc across LNCaP cell models, 22Rv1 cell models, and NEPC patient-derived organoids. **(C)** Results of GSEA performed on the significantly downregulated genes in castrated recipients [Figure 2C]. **(D)** Expression levels of ARv7 signature genes in 22Rv1 xenografts as indicated. Graph depicts the median value between the 25th and 75th percentiles with whiskers indicating the range between the 10th and 90th percentiles. **** $p < 0.0001$, Friedman test.

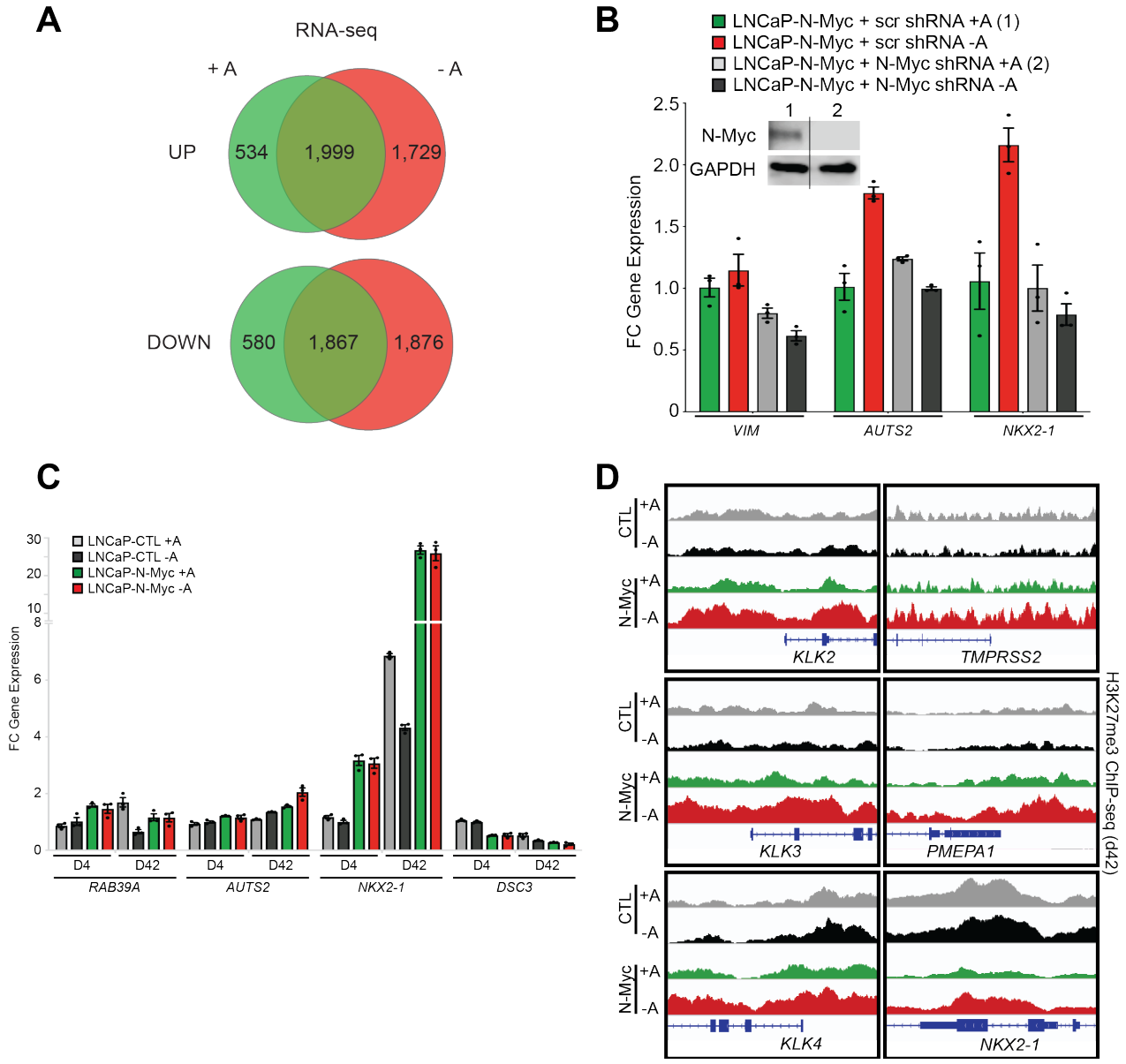

Figure S4. AR signaling alters the N-Myc transcriptome *in vitro*.
(A) Differentially expressed genes (adj. p-value < 0.05) measured by RNA-seq in LNCaP N-Myc cells versus CTL cells as indicated. **(B)** Fold change gene expression based on qRT-PCR data (n = 3 technical replicates per condition) of a known N-Myc target gene (*VIM*) and neural-lineage associated genes (*AUTS2, NKX2-1*), in LNCaP N-Myc cells following knockdown of N-Myc as indicated (see Western Blot inset). Lanes were run on the same gel but were noncontiguous. **(C)** Fold change gene expression of neural (*RAB39A, AUTS2, NKX2-1*) or epithelial (*DSC3*) lineage-associated genes measured by qRT-PCR as indicated (n = 3 technical replicates per condition). **(D)** H3K27me3 levels in the indicated conditions at D42.

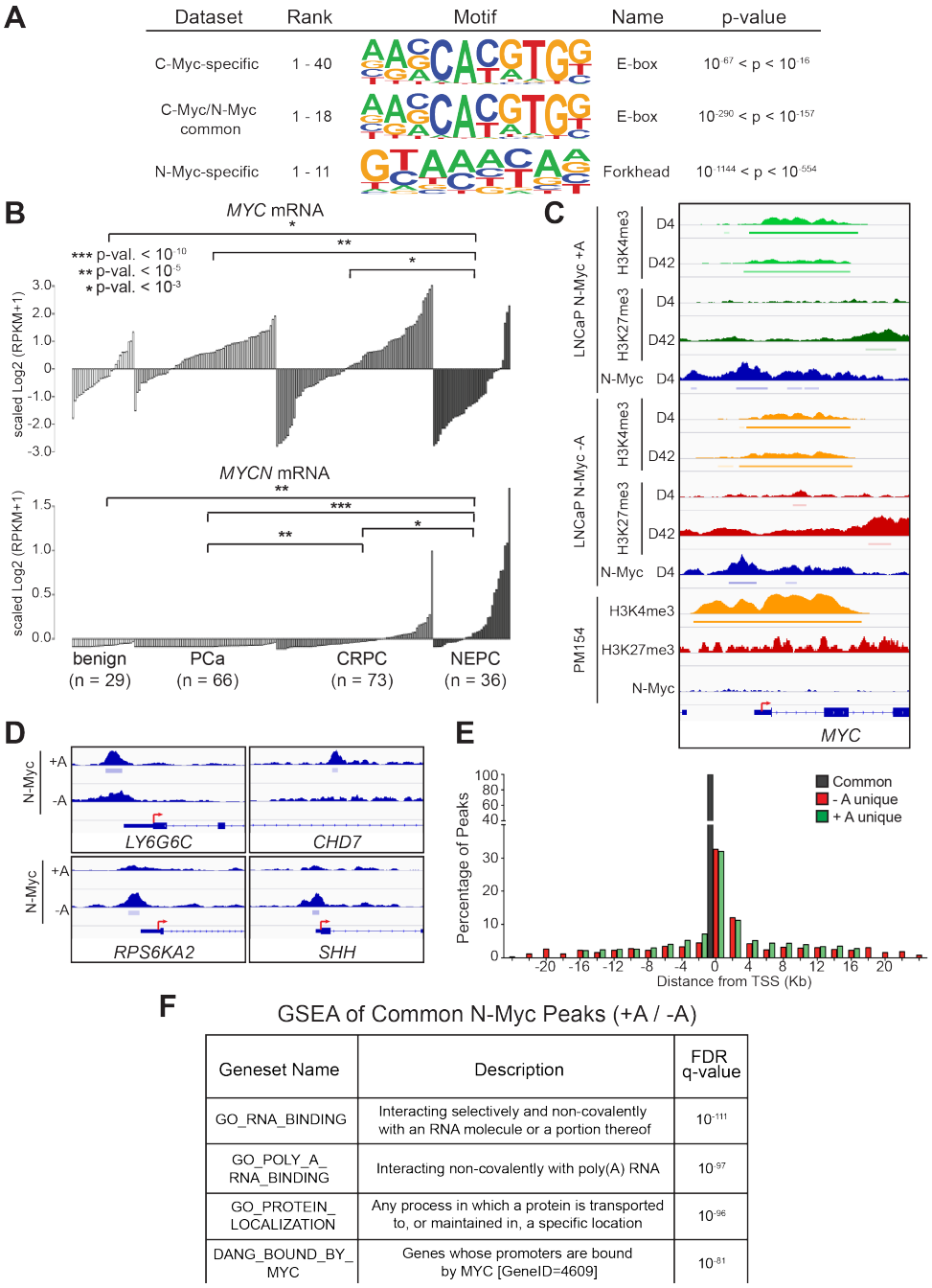

F GSEA of Common N-Myc Peaks (+A / -A)

Geneset Name	Description	FDR q-value
GO_RNA_BINDING	Interacting selectively and non-covalently with an RNA molecule or a portion thereof	10^{-111}
GO_POLY_A_ RNA_BINDING	Interacting non-covalently with poly(A) RNA	10^{-97}
GO_PROTEIN_ LOCALIZATION	Any process in which a protein is transported to, or maintained in, a specific location	10^{-96}
DANG_BOUND_BY_ MYC	Genes whose promoters are bound by MYC [GeneID=4609]	10^{-81}

Figure S5. C-Myc downregulation in cell lines and NEPC patient samples.
(A) Motif analysis performed on C-Myc-specific peaks, N-Myc specific peaks, or C-Myc/N-Myc common peaks in LNCaP cells. Significance determined by hypergeometric test. **(B)** *MYC* and *MYCN* gene expression in benign, PCa, CRPC and NEPC patient samples. Significance determined by Wilcoxon test. **(C)** N-Myc, C-Myc and histone binding at *MYC* locus in the indicated cells and conditions. **(D)** Examples of N-Myc binding sites unique to the presence or absence of androgen. **(E)** Distribution around TSS of N-Myc peaks in indicated conditions. Only the closest 50% of peaks to TSS are shown for clarity. **(F)** Results of GSEA performed on the N-Myc-bound peaks that are common in the presence or absence of androgen and located within 100bp of a TSS.

A

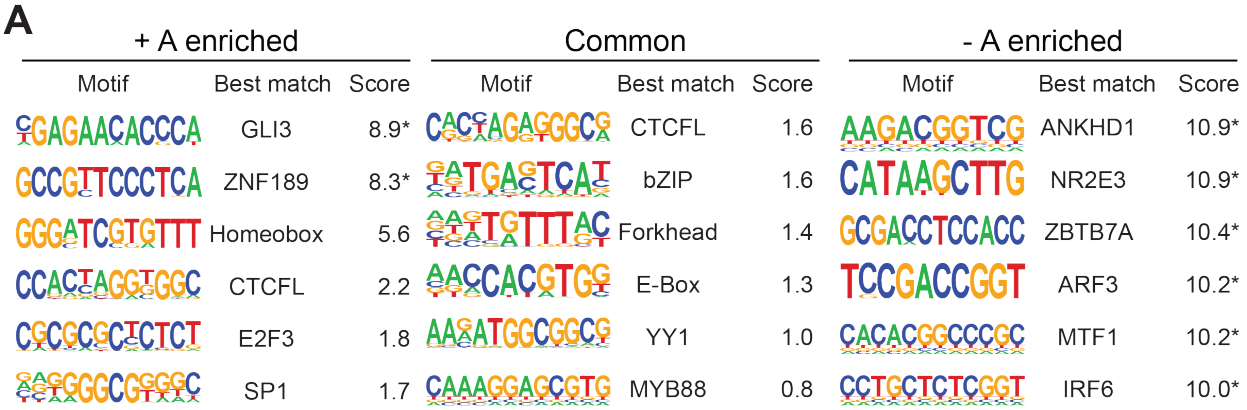

B

	Any AR co-factor (-A only)	Any AR co-factor (+A and -A)	FOXA1 only
GO_POSITIVE_REGULATION_OF_CELL_DIFFERENTIATION		4.98E-14	3.10E-03
GO_EMBRYO_DEVELOPMENT		4.78E-14	1.47E-03
BENPORATH_SOX2_TARGETS	1.46E-04	3.99E-17	
BLALOCK_ALZHEIMERS_DISEASE_UP		2.61E-17	1.95E-04
GO_REGULATION_OF_CELL_DIFFERENTIATION	3.32E-06	8.39E-19	4.19E-04
GO_EPITHELIAL_CELL_DIFFERENTIATION	4.53E-05		
WANG_TUMOR_INVASIVENESS_DN			3.32E-04
GO_NEURON_PROJECTION			4.76E-04
GO_UROGENITAL_SYSTEM_DEVELOPMENT			1.47E-03
MEISSNER_BRAIN_HCP_WITH_H3K4ME3_AND_H3K27ME3	6.01E-05		
GO_NEURON_PART		4.37E-17	5.48E-05
GO_EPITHELIUM_DEVELOPMENT	4.89E-06		
GO_NEUROGENESIS		3.02E-16	
GO_CELL_DEVELOPMENT		3.85E-19	
NUYTTEN_EZH2_TARGETS_UP	4.53E-05		
GO_TISSUE_DEVELOPMENT		1.80E-18	

Figure S6. Characterization of dynamic N-Myc binding sites.
(A) Motif analysis of N-Myc peaks in the indicated conditions. Motifs are listed with their best predicted match to a known protein family**. (B)** Table of FDR q-values of the significantly enriched genesets that were among the top 50 in the GSEA analysis performed for the indicated N-Myc and AR co-factor co-bound genes. Blank cells indicate that the specific geneset did not appear in the top 50 for the indicated GSEA analysis.

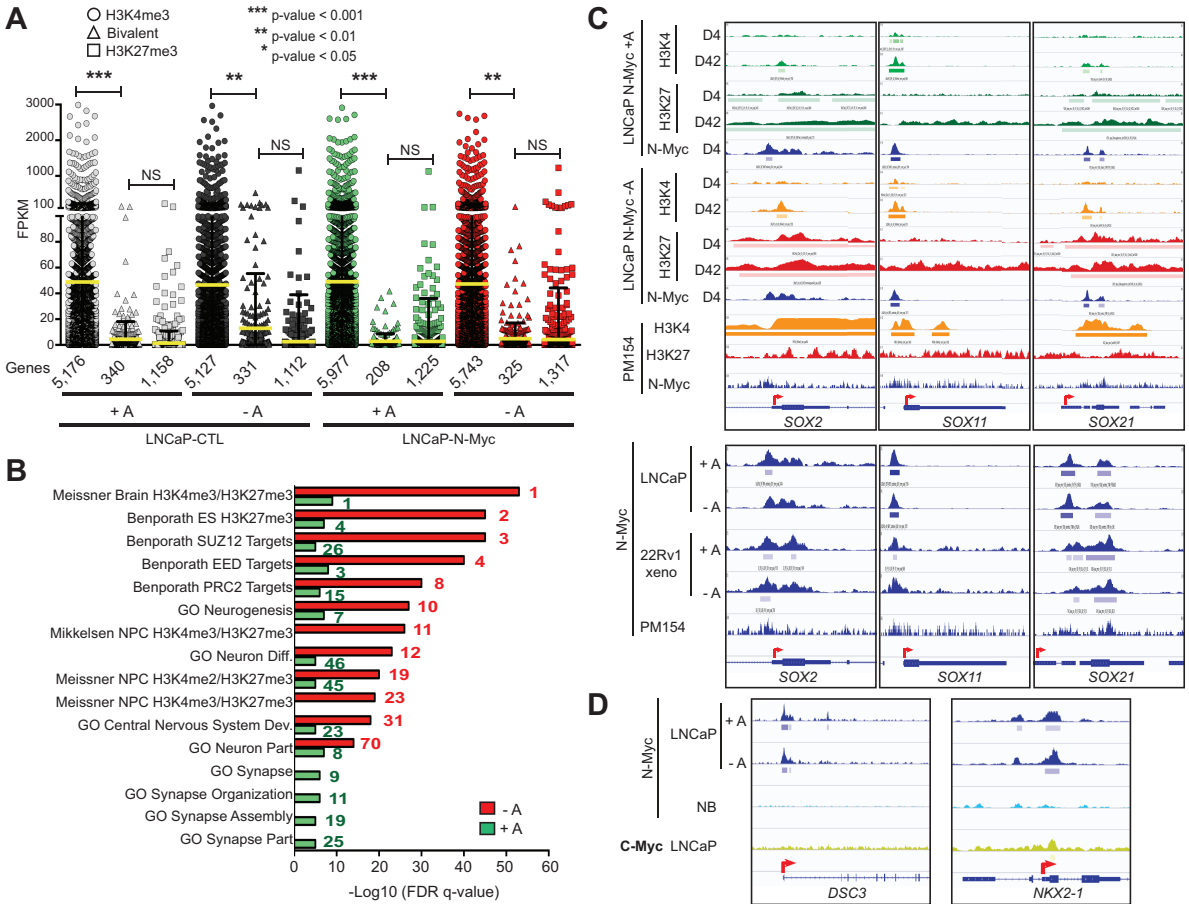

Figure S7. N-Myc regulates bivalency and gene expression.
(A) RNA-seq gene expression of the H3K4me3 only, H3K27me3 only and bivalent marked genes in the indicated cells and conditions. Statistical significance was assessed with Tukey's multiple comparison test. **(B)** GSEA results and ranking of genesets enriched in bivalent and N-Myc bound genes in the indicated conditions. **(C)** ChIP-seq tracks for N-Myc, H3K4me3 and H3K27me3 at the *SOX2*, *SOX11* and *SOX21* loci in the different models and indicated conditions. **(D)** ChIP-seq tracks for N-Myc in LNCaP-N-Myc cells with and without androgen, C-Myc in LNCaP cells with androgen, or N-Myc in BE2C neuroblastoma cells at the indicated genes.

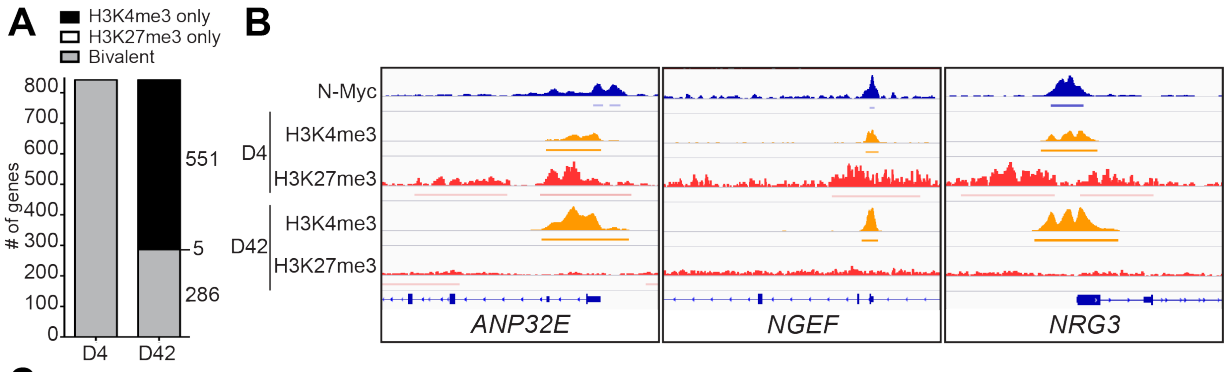

C

Gene Set Name	Genes in Geneset	Genes in Overlap	FDR q-value
MEISSNER_BRAIN_HCP_WITH_H3K4ME3_AND_H3K27ME3	1069	86	4.9E-48
BENPORATH_SUZ12_TARGETS	1038	70	1.56E-33
BENPORATH_ES_WITH_H3K27ME3	1118	72	1.79E-33
BENPORATH_EED_TARGETS	1062	70	3.35E-33
GO_NEUROGENESIS	1402	72	1.94E-27
GO_REGULATION_OF_CELL_DIFFERENTIATION	1492	70	2.58E-24
GO_REGULATION_OF_MULTICELLULAR_ORGANISMAL_DEVELOPMENT	1672	71	3.26E-22
GO_INTRINSIC_COMPONENT_OF_PLASMA_MEMBRANE	1649	70	6.62E-22
DODD_NASOPHARYNGEAL_CARCINOMA_UP	1821	73	1.51E-21
GO_REGULATION_OF_ANATOMICAL_STRUCTURE_MORPHOGENESIS	1021	54	1.03E-20
GO_ORGAN_MORPHOGENESIS	841	49	2.03E-20
BENPORATH_PRC2_TARGETS	652	43	8.99E-20
GO_NEURON_DIFFERENTIATION	874	49	8.99E-20
GOBERT_OLIGODENDROCYTE_DIFFERENTIATION_DN	1080	54	9.9E-20
GO_POSITIVE_REGULATION_OF_MOLECULAR_FUNCTION	1791	69	1.82E-19

Figure S8. Bivalently marked genes at D4 lose H3K27me3 at D42.
(A) Quantification of the number of genes that were bivalently marked and N-Myc bound at D4 [left] and their status at D42 [right] **(B)** ChIP-seq tracks of N-Myc binding, H3K4me3, and H3K27me3 in LNCaP-N-Myc cells at the indicated genes, in the indicated conditions. **(C)** Results of GSEA performed on the 551 genes that were bivalent at D4 but became H3K4me3 only at D42.

3. Specific Aim 3: Determine the impact of the timing of N-Myc on response to NEPC directed therapeutics.

To determine the clinical relevance of these findings, we queried the RNA-seq from our patient cohort and found that the 966 bivalent genes identified in androgen-deprived LNCaP-N-Myc cells successfully classified the PCa, CRPC-Adeno and NEPC patient samples into groups based on NEPC score (**Figure 7A, Figure S9A**) and were enriched in the NEPC samples (**Figure 7B**). The NEPC clinical samples were enriched for neural lineage-associated bivalent genesets compared to PCa or benign samples. These findings also correlated with N-Myc expression level in both NEPC and CRPC-Adeno samples (**Figure 7B**). We observed a stepwise upregulation of the N-Myc-bound and bivalent neural-associated genes during the progression from PCa to NEPC, with upregulation of genes such as *SOX11* and *NKX2-1* and a corresponding downregulation of epithelial lineage-linked genes such as *FGFRL1* and *DSC3* (**Figure 7C, Figure S9B**). This suggests that these genes associated with bivalent marks in N-Myc-expressing cells play a critical role in prostate cancer evolution and may help to identify patients who are most likely to develop NEPC. Lastly, we performed N-Myc ChIP-seq in the patient-

derived NEPC organoid PM154 and found that, despite fewer numbers of total peaks, 79% of the peaks were in common with LNCaP-N-Myc and 22Rv1-N-Myc xenografts, including neural lineage-associated genes (*NREP, ULK2, RAB39A*), bivalent genes (*RAB39A*), and the H3K27me3 writer *EZH2* (**Figure S9C,D**). Moreover, we confirmed the N-Myc-dependent upregulation of these bivalent genes in 22Rv1 xenografts and NEPC patient-derived organoid models (**Figure S9E**).

We have previously shown that, in the context of active AR signaling, N-Myc cooperates with EZH2 and redirects its activity to downregulate AR target genes [6]. Using an *in situ* proximity ligation assay (PLA) to monitor EZH2 and N-Myc complex formation, we confirmed the presence of the EZH2/N-Myc complexes in LNCaP and 22Rv1-N-Myc cells with and without an active AR-signaling and in an AR-negative, NEPC patient-derived organoid (PM154, **Figure S9F**). This suggests that N-Myc and EZH2 maintain a protein-protein interaction in the absence of AR that may regulate the H3K27me3 status of the bivalent genes. To address this, we performed shRNA-mediated knockdown of EZH2 in PM154 cells. After validation on genes that have been previously shown to be regulated by EZH2, we observed that knockdown of EZH2 led to a dramatic upregulation of the bivalent genes that were previously downregulated by N-Myc and inversely (**Figure 7D**). In addition to shRNA strategies, PM154 cells were also treated with a pharmacologic EZH2 inhibitor (GSK503). Targeted GSEA demonstrated a significant de-enrichment of multiple neural lineage-associated bivalent genesets (**Figure 7B, Figure S9G**).

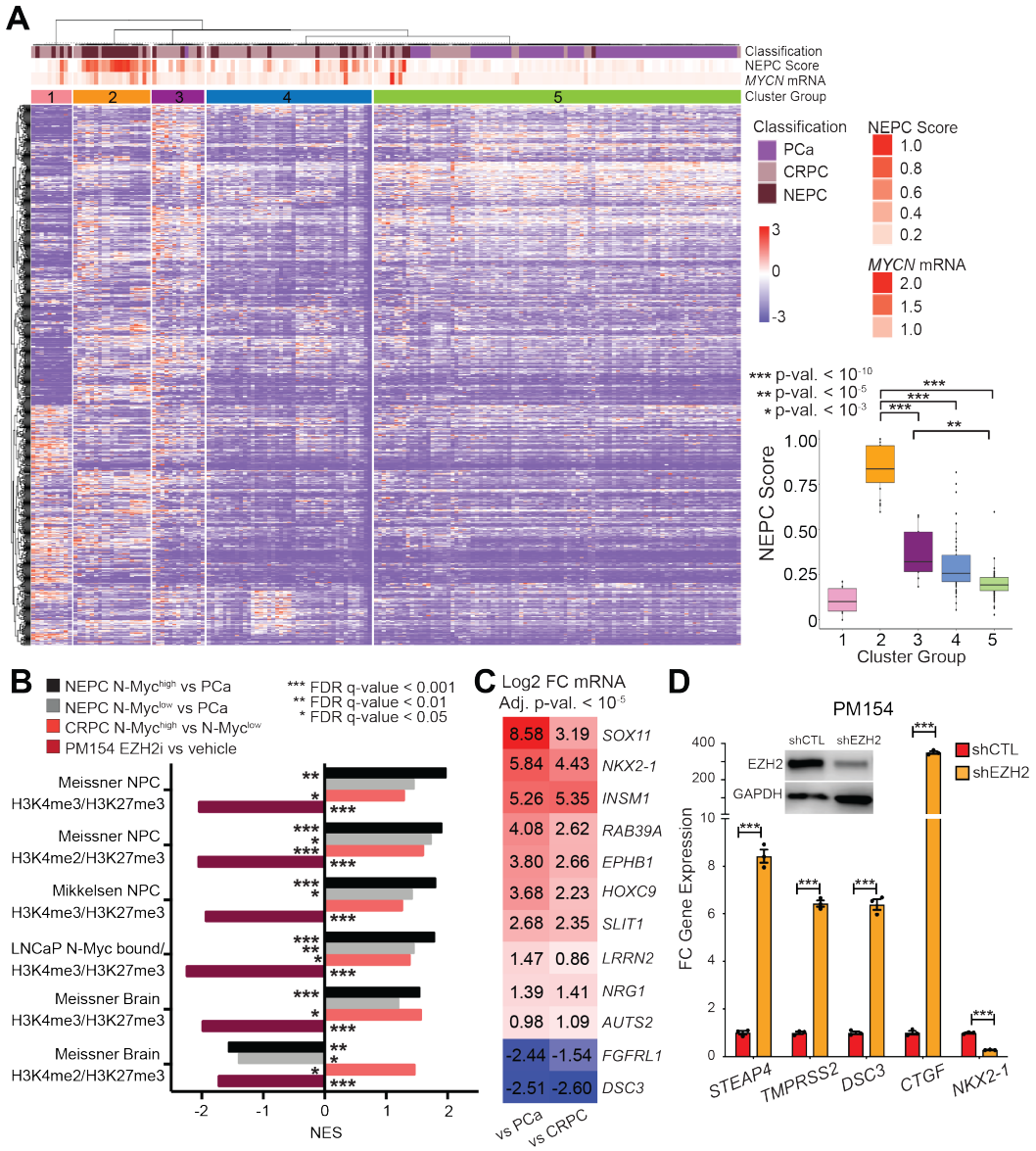

Figure 7. N-Myc-induced bivalent genes are clinically relevant.

(A) [Top] Unsupervised clustering of PCa (n = 66), CRPC (n = 73) and NEPC (n = 36) patient samples based on the expression level of the 966 bivalent and N-Myc bound genes in LNCaP-N-Myc cells at D4 without androgen. [Bottom] NEPC score for each cluster group. Graph depicts the median value between the 25th and 75th percentiles with whiskers indicating the range within 1.5 IQR, Student's unpaired two-tailed t-test. **(B)** Targeted GSEA of bivalent-related genesets in the five NEPC samples with the highest (N-Myc^{high}) or lowest (N-Myc^{low}) level of *MYCN* expression versus PCa (n = 66) patient samples, on the five CRPC with the highest level of *MYCN* expression versus the five lowest, and on PM154 cells treated with an EZH2 inhibitor versus vehicle. **(C)** Heatmap of log2(fold change) of genes in NEPC (n = 36) versus PCa (n = 66) or NEPC versus CRPC (n = 73) patient samples. Illustrated genes are bivalent and bound by N-Myc in LNCaP-N-Myc cells without androgen at D4. **(D)** Fold change expression of the indicated genes based on qRT-PCR data (n = 3 technical replicates) in PM154 following EZH2 knockdown (see Western Blot inset). *** p < 0.001, Student's unpaired two-tailed t-test.

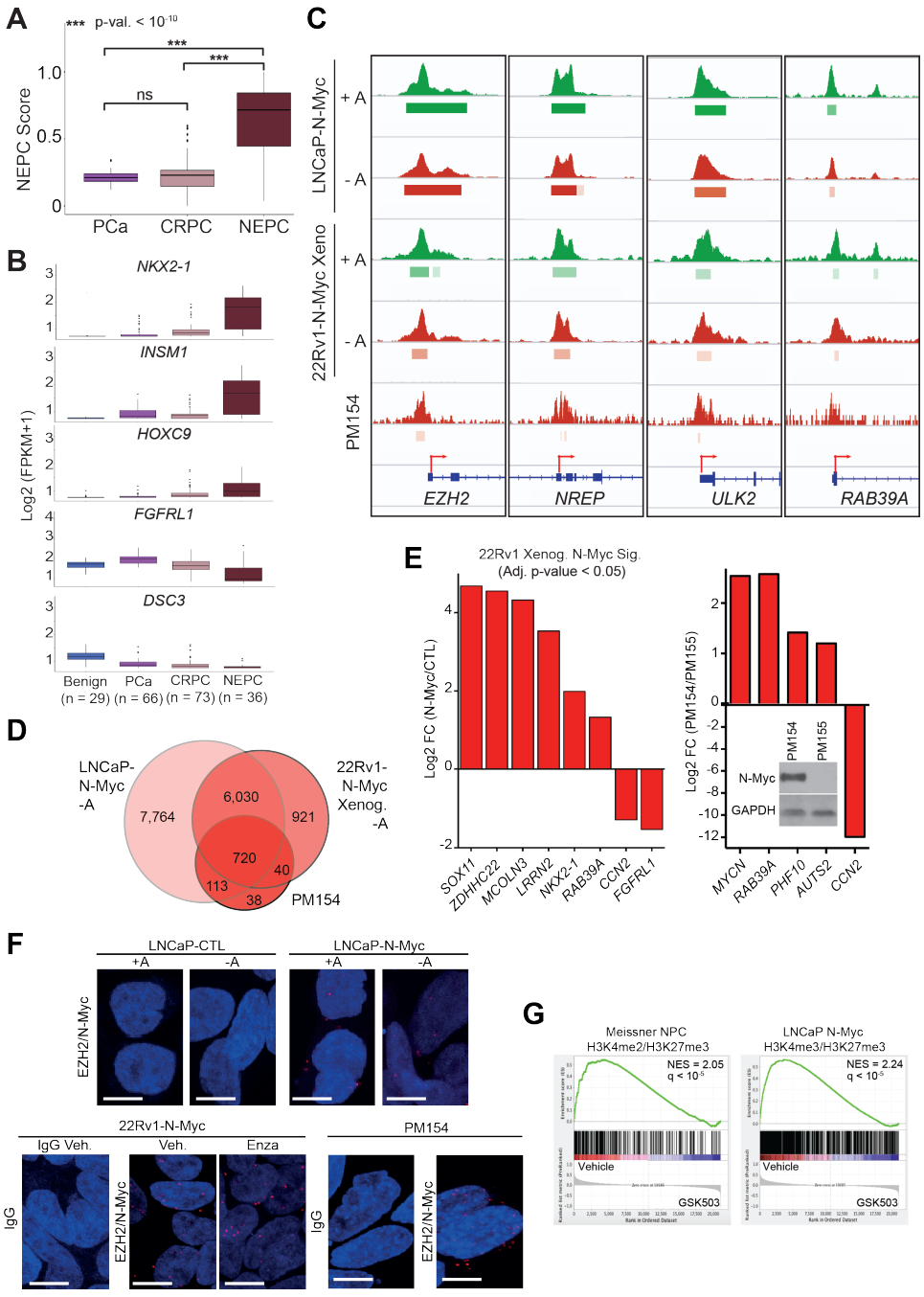

Figure S9. Validation of N-Myc induced bivalent genes in models and patient samples.
(A) Distribution of NEPC Score across PCa, CRPC and NEPC patients. Graph depicts the median value between the 25th and 75th percentiles with whiskers indicating the range within 1.5 IQR, Student's unpaired two-tailed t test. **(B)** Box plots of the mRNA expression for the indicated genes in benign, PCa, CRPC and NEPC clinical samples. **(C)** ChIP-seq tracks of N-Myc binding in LNCaP-N-Myc (n = 2 biological replicates per condition), 22Rv1-N-Myc xenografts (n = 2 biological replicates per condition) and PM154 cells at the indicated genes, in the indicated conditions. **(D)** Overlap of the numbers of genes bound by N-Myc in LNCaP-N-Myc, 22Rv1-N-Myc and PM154 cells. **(E)** Log2 fold change (N-Myc vs CTL xenografts from castrated mice, left) and log2 fold change (PM154 versus PM155, right) of indicated genes after validation of N-Myc expression by Western Blot (see inset). **(F)** Proximity ligation assay showing EZH2 and N-Myc interactions in the indicated cells and conditions (scale bar = 5 µm). **(G)**

Enrichment plots of the Meissner NPC H3K4me2/H3K27me3 and LNCaP N-Myc bivalent genesets from PM154 cells in the indicated conditions.

What opportunities for training and professional development has the project provided?

Drs Beltran and Rickman are fully committed to furthering the training and professional development of the post-doctoral fellows and students affiliated to this project. This has including presentations at the AACR – Prostate Cancer December 2017, Orlando, FL; Prostate Cancer SPORE programs Annual Retreat, February 2018, 2019 Ft. Lauderdale, FL; AACR April 2018, 2019; Society of Basic Urologic Research, Palm Beach, CA Nov 2018 and New Orleans, LA, Nov 2019. Nick Brady (postdoctoral fellow in the Rickman lab) received prize for best abstract at the; Prostate Cancer SPORE program Annual Retreat, February 2019 .

Postdoc fellows also participate in the following:
NIH T32 MTOR Course. 15 lectures, especially designed for MTOR, will be presented by our preceptors jointly with their clinical collaborators to showcase the principles of translational cancer research and team science.

Transitioning to Research Independence seminar series. A seminar series geared towards postdoctoral researchers and fellows who plan to set up their own laboratory and develop their own research program at an academic institution. Trainees will comprehend the faculty application process; understand strategies for funding, mentoring and leadership to effectively run their own research group.

Biostatistics Lecture Series through the Clinical and Translational Science Center. This is a monthly lecture series geared towards clinical investigators, research staff, and students who are interested in gaining insight into fundamental research design and statistical concepts with a focus on practical knowledge.

We presented this initial data at the Multi-institutional Prostate Cancer Meeting in Ft Lauderdale in February 2018 which is organized and led by the SPORE programs as an oral presentation as well as an oral presentation at the same meeting in 2019. This data was also presented at AACR – Prostate Cancer December 2017, Orlando, FL; Prostate Cancer SPORE programs Annual Retreat, march 2018, Ft. Lauderdale, FL; AACR April 2018; The Prostate Cancer Foundation Annual Retreat, 2019, Society of Basic Urologic Research, Palm Beach, CA Nov 2018 and New Orleans, LA, Nov 2019. The following manuscripts are related to this project:

1. Puca, L., et al., Patient derived organoids to model rare prostate cancer phenotypes. Nat Commun, 2018. 9(1): p. 2404.

2. Beltran, H., et al., A phase II trial of the aurora kinase A inhibitor alisertib for patients with castration resistant and neuroendocrine prostate cancer: efficacy and biomarkers. Clin Cancer Res, 2018.

3. Puca L, Gayvert K Sailor V, Conteduca V, Dardenne E, Sigouros M, Isse K, Kearney M, Vosoughi A, Pan H, Motangagh S, Hess J, Sboner A, Wang Y, Dittamore R, Rickman D, Nanus DM, Tagawa ST, Elemento O, Mosquera JM, Saunders L, Beltran H. Delta like protein 3 expression and therapeutic targeting in neuroendocrine prostate cancer, Science Translational Medicine, 2019

4. Berger A, Brady NJ, Bareja R, Dardenne E, Robinson B, Vincenza Conteduca V, Augello MA, Ahmed A, Puca L, Hwang I, Bagadion AM, Sboner A, Elemento O, Paik J, Barbieri CE, Dephoure N, Beltran H and Rickman DS. N-Myc-mediated epigenetic reprogramming drives lineage plasticity in advanced prostate cancer. Journal of Clinical Investigation, 2019 Jul 1;130:3924-3940

4. Nicholas J. Brady, Alyssa M. Bagadion, Richa Singh, Vincenza Conteduca, Elisa Arceci, Francesca Khani, Kate Dunmore, Lucie Van Emmenis, Michael Sigouros, Rohan Bareja, Andrea Sboner, Olivier Elemento, David Nanus, Massimo Loda, Himisha Beltran, Brian Robinson and David S. Rickman. Single-Cell Assessment of the Synergy between N-Myc Overexpression and RB1 Loss-of-Function in NEPC (in preparation).

What do you plan to do during the next reporting period to accomplish the goals?
If this is the final report, state "Nothing to Report."

Related to Aim 1, we continue to recruit CRPC and NEPC patients for this study. Given the limited availability of fresh/frozen samples especially of archival primary tumors, we have been developing a custom-designed targeted mRNA assay to evaluate N-myc target gene expression amenable to formalin fixed paraffin embedded tissue samples using Nanostring approach (an approach previously described - Beltran et al, CCR 2017). This will allow for assessment of dynamic changes in N-Myc and N-Myc target gene expression, AURKA, EZH2, and other genes during disease progression towards the NEPC phenotype. We will correlate these changes with genomics (including TP53 and RB1 loss). We continue ongoing analyses of clinical cohorts with outcomes data including MLN8327 trial patients (pre-treatment and progression biopsies), pre-treatment biopsies CRPC patients treated with abi/enza (SU2C-PCF Dream Team cohort of 500 patients, in process) and localized cohorts including those with GenomeDx data and an addition cohort from CALGB90203 (nanostring data in process).

Related to Aim 2, we will continue our analyses of the N-Myc cistrome and how N-Myc impacts transcriptomic reprogramming interacting co-factors that account for the induction of a lineage plastic state that favors the development of NEPC in our models (GEM, xenograft, cell lines and patient-derived NEPC organoids). We will perform genetic experiments (knock-in/knock-out) of specific cofactors to determine their cooperative role with N-Myc in driving this phenotype. We are also performing ChIPseq using human samples. We will also be further exploring the role of N-Myc on epigenomic reprogramming and how this enables the lineage plasticity phenotype.

Related to Aim 3, we will, focus on compounds that have been shown to be stable in animals. In addition to early stage drug development, we are also exploring additional opportunities for clinical trial development for NEPC, specifically around EZH2, given number of new EZH2i drugs now in later stages development (Pfizer, Eli Lilly, Constellation, Epizyme, GSK).

4. **IMPACT:** Describe distinctive contributions, major accomplishments, innovations, successes, or any change in practice or behavior that has come about as a result of the project relative to:

What was the impact on the development of the principal discipline(s) of the project?
If there is nothing significant to report during this reporting period, state "Nothing to Report."

Despite recent advances in the development of highly effective AR-directed therapies for the treatment of prostate cancer, acquired resistance ultimately ensues. Since AR-indifferent prostate cancer is thought to arise and evolve in the face of hormonal therapy, there is concern that the development of more potent AR-targeted treatments will increase the incidence of this lethal form of prostate cancer. Lineage plasticity as a mechanism of resistance to targeted therapies has been implicated in both epithelial tumors and leukemias, suggesting that significant findings may successfully translate to additional tumor types [10-17]. A recently published study using a machine-learning approach has identified a link between stemness and what is termed oncogenic dedifferentiation [18].

Here, we present data that highlights how an oncogenic transcription factor, N-Myc, can promote the acquisition of alternative lineage identities, including stem-like precursor states of

the neural lineage, and explains the progression of dedifferentiation steps required during disease progression[19]. We show that N-Myc functions in the epigenomic and transcriptomic reprogramming of prostate cancer epithelial cells in an androgen-dependent manner. Data from in vivo models revealed that N-Myc driven prostate tumors are more aggressive following castration, including the development of metastatic lesions and the aberrant acquisition of alternative lineage programs. Whether or not these changes involve a transient, undifferentiated stem-like state [12,13,20] or a direct transdifferentiation [17] and the role of the local microenvironment in dictating the choice of lineage remains to be elucidated.

The N-Myc-induced transcriptomic landscape also changed dramatically in vivo following castration. Integrative ChIP-seq/RNA-seq data revealed a rapid, androgen-dependent change in the N-Myc cistrome, transcriptome, and histone methylation. In the presence of androgen, N-Myc binds to regulatory sequences associated with AR binding, upstream of AR target genes, to suppress gene expression. Consistent with the overlap between AR and N-Myc binding, forkhead box and homeobox consensus motifs were significantly enriched in chromatin regions directly bound by N-Myc. Moreover, FOXA1 binding was associated with androgen-dependent changes in the N-Myc binding at genes associated with the neural lineage and was essential for N-Myc binding at the loci tested, including *NKX2-1* which has been implicated in neuroendocrine-like small cell lung cancers [21]. Proteomic data confirmed an interaction between chromatin-bound N-Myc and the AR co-factor HOXB13, as well as identified interactions with the heterochromatin-associated proteins CBX1/3/5. Recent studies have implicated CBX3 in neural lineage specification, which could cooperate with N-Myc to facilitate lineage plasticity [22]. In the absence of androgen, the N-Myc cistrome is re-directed towards promoters of genes expressed in neural precursors/NSC and is associated with transcriptional activation and reprogramming of epigenetic H3K4me3/H3K27me3 bivalent marks at neural lineage-associated genes. Finally, using proteomic approaches, we identified a number of previously uncharacterized N-Myc-interacting proteins that will provide potential targets to inform future studies of Myc-driven cancers.

Another important finding from this study came from our direct cistromic comparison of N-Myc and its related family member C-Myc in prostate cancer or N-Myc in neuroblastoma. The C-Myc locus is commonly amplified in early prostate cancer development [23] and we show that its expression decreases during disease progression. This may be partially explained by the deposition of H3K27me3 marks in the gene body following long-term androgen withdrawal (**Figure S5C**). Interestingly, a recent report suggested that, in a specific genetic context (Rb1/Trp53 loss; AKT; BCL2 induction), C-Myc expression in prostate basal cells leads to the development of NEPC [21]. We found that in LNCaP cells (*RB1* and *TP53* wild type), 49% of N-Myc binding does not overlap with C-Myc binding. We also found that these N-Myc-specific sites are enriched for genes associated with the neural lineage. Altogether, this suggests that N-Myc and C-Myc share common functions but N-Myc may also regulate molecular programs that are not driven by C-Myc in prostate cancer cells. This is consistent with other data from prostate cancer [23-26] as well as several other solid tumors, such as lung [27-33] and pancreas [34-36].

Our studies have identified a potential mechanism by which N-Myc overexpression and its subsequent DNA binding induce epigenomic and transcriptomic reprogramming resulting in a castration-resistant, lineage plastic phenotype that gives rise to NEPC. These data provide new insights into the early events of lineage switching as a mechanism of escape to the effects of hormone therapy in prostate cancer. More intriguingly, the changes that occur in the face of AR targeted therapy may also provide a molecular signature to classify prostate cancer patients and potentially help predict those approximately 20% of CRPC patients that may eventually develop NEPC [37,38]. Clinical trials have been developed for patients with NEPC, targeting Aurora Kinase, Notch and PD-1 pathways (NCT01799278, NCT02709889, NCT03179410). Additionally, EZH2

inhibitors have entered early stage clinical trials in patients with a wide range of tumor types (NCT03525795, NCT02860286), including prostate (NCT03480646). Identifying the patients most at-risk of developing NEPC could provide opportunities for earlier clinical intervention and allow for inclusion in future clinical trials of these novel targeted therapies in NEPC.

References

1 Epstein, J. I. *et al.* Proposed morphologic classification of prostate cancer with neuroendocrine differentiation. *Am J Surg Pathol* **38**, 756-767, doi:10.1097/PAS.0000000000000208 (2014).

2 Lee, G. *et al.* Isolation and directed differentiation of neural crest stem cells derived from human embryonic stem cells. *Nat Biotechnol* **25**, 1468-1475, doi:10.1038/nbt1365 (2007).

3 Subramanian, A. *et al.* Gene set enrichment analysis: a knowledge-based approach for interpreting genome-wide expression profiles. *Proc Natl Acad Sci U S A* **102**, 15545-15550, doi:10.1073/pnas.0506580102 (2005).

4 Bhattacharya, B. *et al.* Gene expression in human embryonic stem cell lines: unique molecular signature. *Blood* **103**, 2956-2964, doi:10.1182/blood-2003-09-3314 (2004).

5 Dulken, B. W., Leeman, D. S., Boutet, S. C., Hebestreit, K. & Brunet, A. Single-Cell Transcriptomic Analysis Defines Heterogeneity and Transcriptional Dynamics in the Adult Neural Stem Cell Lineage. *Cell Rep* **18**, 777-790, doi:10.1016/j.celrep.2016.12.060 (2017).

6 Dardenne, E. *et al.* N-Myc Induces an EZH2-Mediated Transcriptional Program Driving Neuroendocrine Prostate Cancer. *Cancer Cell* **30**, 563-577, doi:10.1016/j.ccell.2016.09.005 (2016).

7 Meissner, A. *et al.* Genome-scale DNA methylation maps of pluripotent and differentiated cells. *Nature* **454**, 766-770, doi:10.1038/nature07107 (2008).

8 Mikkelsen, T. S. *et al.* Genome-wide maps of chromatin state in pluripotent and lineage-committed cells. *Nature* **448**, 553-560, doi:10.1038/nature06008 (2007).

9 Mohammed, H. *et al.* Rapid immunoprecipitation mass spectrometry of endogenous proteins (RIME) for analysis of chromatin complexes. *Nat Protoc* **11**, 316-326, doi:10.1038/nprot.2016.020 (2016).

10 Beltran, H. *et al.* Divergent clonal evolution of castration-resistant neuroendocrine prostate cancer. *Nat Med* **22**, 298-305, doi:10.1038/nm.4045 (2016).

11 Haddox, C. L. *et al.* Blinatumomab-induced lineage switch of B-ALL with t(4:11)(q21;q23) KMT2A/AFF1 into an aggressive AML: pre- and post-switch phenotypic, cytogenetic and molecular analysis. *Blood Cancer J* **7**, e607, doi:10.1038/bcj.2017.89 (2017).

12 Ku, S. Y. *et al.* Rb1 and Trp53 cooperate to suppress prostate cancer lineage plasticity, metastasis, and antiandrogen resistance. *Science* **355**, 78-83, doi:10.1126/science.aah4199 (2017).

13 Mu, P. *et al.* SOX2 promotes lineage plasticity and antiandrogen resistance in TP53- and RB1-deficient prostate cancer. *Science* **355**, 84-88, doi:10.1126/science.aah4307 (2017).

14 Rickman, D. S., Beltran, H., Demichelis, F. & Rubin, M. A. Biology and evolution of poorly differentiated neuroendocrine tumors. *Nat Med* **23**, 1-10, doi:10.1038/nm.4341 (2017).

15 Sequist, L. V. *et al.* Genotypic and histological evolution of lung cancers acquiring resistance to EGFR inhibitors. *Sci Transl Med* **3**, 75ra26, doi:10.1126/scitranslmed.3002003 (2011).
16 Tata, P. R. *et al.* Developmental History Provides a Roadmap for the Emergence of Tumor Plasticity. *Developmental cell* **44**, 679-693 e675, doi:10.1016/j.devcel.2018.02.024 (2018).
17 Zou, M. *et al.* Transdifferentiation as a Mechanism of Treatment Resistance in a Mouse Model of Castration-resistant Prostate Cancer. *Cancer Discov*, doi:10.1158/2159-8290.CD-16-1174 (2017).
18 Malta, T. M. *et al.* Machine Learning Identifies Stemness Features Associated with Oncogenic Dedifferentiation. *Cell* **173**, 338-354 e315, doi:10.1016/j.cell.2018.03.034 (2018).
19 Berger, A. *et al.* N-Myc-mediated epigenetic reprogramming drives lineage plasticity in advanced prostate cancer. *J Clin Invest* **130**, doi:10.1172/JCI127961 (2019).
20 Smith, B. A. *et al.* A Human Adult Stem Cell Signature Marks Aggressive Variants across Epithelial Cancers. *Cell Rep* **24**, 3353-3366 e3355, doi:10.1016/j.celrep.2018.08.062 (2018).
21 Park, J. W. *et al.* Reprogramming normal human epithelial tissues to a common, lethal neuroendocrine cancer lineage. *Science* **362**, 91-95, doi:10.1126/science.aat5749 (2018).
22 Huang, C. *et al.* Cbx3 maintains lineage specificity during neural differentiation. *Genes Dev* **31**, 241-246, doi:10.1101/gad.292169.116 (2017).
23 Gurel, B. *et al.* Nuclear MYC protein overexpression is an early alteration in human prostate carcinogenesis. *Mod Pathol* **21**, 1156-1167, doi:modpathol2008111 [pii] 10.1038/modpathol.2008.111 (2008).
24 Clegg, N. J. *et al.* MYC cooperates with AKT in prostate tumorigenesis and alters sensitivity to mTOR inhibitors. *PLoS One* **6**, e17449, doi:10.1371/journal.pone.0017449 (2011).
25 Ellwood-Yen, K. *et al.* Myc-driven murine prostate cancer shares molecular features with human prostate tumors. *Cancer Cell* **4**, 223-238 (2003).
26 Koh, C. M. *et al.* MYC and Prostate Cancer. *Genes Cancer* **1**, 617-628, doi:10.1177/1947601910379132 10.1177_1947601910379132 [pii] (2010).
27 Huijbers, I. J. *et al.* Rapid target gene validation in complex cancer mouse models using re-derived embryonic stem cells. *EMBO Mol Med* **6**, 212-225, doi:10.1002/emmm.201303297 (2014).
28 Kim, D. W. *et al.* Genetic requirement for Mycl and efficacy of RNA Pol I inhibition in mouse models of small cell lung cancer. *Genes Dev* **30**, 1289-1299, doi:10.1101/gad.279307.116 (2016).
29 Mollaoglu, G. *et al.* MYC Drives Progression of Small Cell Lung Cancer to a Variant Neuroendocrine Subtype with Vulnerability to Aurora Kinase Inhibition. *Cancer Cell* **31**, 270-285, doi:10.1016/j.ccell.2016.12.005 (2017).
30 Peifer, M. *et al.* Integrative genome analyses identify key somatic driver mutations of small-cell lung cancer. *Nat Genet* **44**, 1104-1110, doi:10.1038/ng.2396 (2012).
31 Rudin, C. M. & Poirier, J. T. MYC, MAX, and small cell lung cancer. *Cancer discovery* **4**, 273-274, doi:10.1158/2159-8290.CD-14-0069 (2014).

32 Sos, M. L. *et al.* A framework for identification of actionable cancer genome dependencies in small cell lung cancer. *Proc Natl Acad Sci U S A* **109**, 17034-17039, doi:10.1073/pnas.1207310109 (2012).
33 Wong, A. J. *et al.* Gene amplification of c-myc and N-myc in small cell carcinoma of the lung. *Science* **233**, 461-464 (1986).
34 Bergmann, F. *et al.* Acinar cell carcinomas of the pancreas: a molecular analysis in a series of 57 cases. *Virchows Arch* **465**, 661-672, doi:10.1007/s00428-014-1657-8 (2014).
35 Fielitz, K. *et al.* Characterization of pancreatic glucagon-producing tumors and pituitary gland tumors in transgenic mice overexpressing MYCN in hGFAP-positive cells. *Oncotarget*, doi:10.18632/oncotarget.12766 (2016).
36 Skoudy, A., Hernandez-Munoz, I. & Navarro, P. Pancreatic ductal adenocarcinoma and transcription factors: role of c-Myc. *J Gastrointest Cancer* **42**, 76-84, doi:10.1007/s12029-011-9258-0 (2011).
37 Aggarwal, R. *et al.* Clinical and Genomic Characterization of Treatment-Emergent Small-Cell Neuroendocrine Prostate Cancer: A Multi-institutional Prospective Study. *J Clin Oncol*, JCO2017776880, doi:10.1200/JCO.2017.77.6880 (2018).
38 Bluemn, E. G. *et al.* Androgen Receptor Pathway-Independent Prostate Cancer Is Sustained through FGF Signaling. *Cancer Cell* **32**, 474-489 e476, doi:10.1016/j.ccell.2017.09.003 (2017).

What was the impact on other disciplines?
If there is nothing significant to report during this reporting period, state "Nothing to Report."

Describe how the findings, results, or techniques that were developed or improved, or other products from the project made an impact or are likely to make an impact on other disciplines.

Results from this study may provide insights in other cancer types that develop lineage plasticity as a resistance mechanism to targeted therapies (eg., EGFR mutated lung adenocarcinomas that transform to small cell carcinoma), as there are shared molecular features and potentially shared therapeutic implications.

What was the impact on technology transfer?
If there is nothing significant to report during this reporting period, state "Nothing to Report."

Nothing to report.

What was the impact on society beyond science and technology?
If there is nothing significant to report during this reporting period, state "Nothing to Report."

Describe how results from the project made an impact, or are likely to make an impact, beyond the bounds of science, engineering, and the academic world on areas such as:

- *improving public knowledge, attitudes, skills, and abilities;*
- *changing behavior, practices, decision making, policies (including regulatory policies), or social actions; or*
- *improving social, economic, civic, or environmental conditions.*

Nothing to report.

5. **CHANGES/PROBLEMS:** The Project Director/Principal Investigator (PD/PI) is reminded that the recipient organization is required to obtain prior written approval from the awarding agency Grants Officer whenever there are significant changes in the project or its direction. If not previously reported in writing, provide the following additional information or state, "Nothing to Report," if applicable:

Changes in approach and reasons for change

Describe any changes in approach during the reporting period and reasons for these changes. Remember that significant changes in objectives and scope require prior approval of the agency.

No changes/problems to report

Actual or anticipated problems or delays and actions or plans to resolve them

Describe problems or delays encountered during the reporting period and actions or plans to resolve them.

Nothing to report.

Changes that had a significant impact on expenditures

Describe changes during the reporting period that may have had a significant impact on expenditures, for example, delays in hiring staff or favorable developments that enable meeting objectives at less cost than anticipated.

Nothing to report.

Significant changes in use or care of human subjects, vertebrate animals, biohazards, and/or select agents

Describe significant deviations, unexpected outcomes, or changes in approved protocols for the use or care of human subjects, vertebrate animals, biohazards, and/or select agents during the reporting period. If required, were these changes approved by the applicable institution committee (or equivalent) and reported to the agency? Also specify the applicable Institutional Review Board/Institutional Animal Care and Use Committee approval dates.

Significant changes in use or care of human subjects

Nothing to report.

Significant changes in use or care of vertebrate animals.

Nothing to report.

Significant changes in use of biohazards and/or select agents

Nothing to report.

there is nothing to report under a particular item, state "Nothing to Report."

- **Publications, conference papers, and presentations**
  Report only the major publication(s) resulting from the work under this award.

  Journal publications.

  1. Puca, L., et al., Patient derived organoids to model rare prostate cancer phenotypes. Nat Commun, 2018. **9**(1): p. 2404; yes

  2. Beltran, H., et al., A phase II trial of the aurora kinase A inhibitor alisertib for patients with castration resistant and neuroendocrine prostate cancer: efficacy and biomarkers. Clin Cancer Res, 2018; yes

  3. Berger A, Brady NJ, Bareja R, Dardenne E, Robinson B, Vincenza Conteduca V, Augello MA, Ahmed A, Puca L, Hwang I, Bagadion AM, Sboner A, Elemento O, Paik J, Barbieri CE, Dephoure N, Beltran H and Rickman DS. N-Myc-mediated epigenetic reprogramming drives lineage plasticity in advanced prostate cancer. Journal of Clinical Investigation, 2019 Jul 1;130:3924-3940., yes

  4. Nicholas J. Brady, Alyssa M. Bagadion, Richa Singh, Vincenza Conteduca, Elisa Arceci, Francesca Khani, Kate Dunmore, Lucie Van Emmenis, Michael Sigouros, Rohan Bareja, Andrea Sboner, Olivier Elemento, David Nanus, Massimo Loda, Himisha Beltran, Brian Robinson and David S. Rickman. Single-Cell Assessment of the Synergy between N-Myc Overexpression and RB1 Loss-of-Function in NEPC (in preparation). Yes, to a small degree

Books or other non-periodical, one-time publications.

Nothing to report.

Other publications, conference papers, and presentations. *Identify any other publications, conference papers and/or presentations not reported above. Specify the status of the publication as noted above. List presentations made during the last year (international, national, local societies, military meetings, etc.). Use an asterisk (*) if presentation produced a manuscript.*

We presented this data at the AACR – Prostate Cancer December 2017, Orlando, FL; Prostate Cancer SPORE programs Annual Retreat, February 2018, 2019 Ft. Lauderdale, FL; AACR April 2018, 2019; Society of Basic Urologic Research, Palm Beach, CA Nov 2018 and New Orleans, LA, Nov 2019.

- **Website(s) or other Internet site(s)**
  List the URL for any Internet site(s) that disseminates the results of the research activities. A short description of each site should be provided. It is not necessary to include the publications already specified above in this section.

Nothing to report.

- **Technologies or techniques**
  Identify technologies or techniques that resulted from the research activities. In addition to a description of the technologies or techniques, describe how they will be shared.

Nothing to report.

- **Inventions, patent applications, and/or licenses**
  Identify inventions, patent applications with date, and/or licenses that have resulted from the research. State whether an application is provisional or non-provisional and indicate the application number. Submission of this information as part of an interim research performance progress report is not a substitute for any other invention reporting required under the terms and conditions of an award.

Nothing to report.

- **Other Products**

  Identify any other reportable outcomes that were developed under this project. Reportable outcomes are defined as a research result that is or relates to a product, scientific advance, or research tool that makes a meaningful contribution toward the understanding, prevention, diagnosis, prognosis, treatment, and/or rehabilitation of a disease, injury or condition, or to improve the quality of life. Examples include:

  - *data or databases;*
  - *biospecimen collections;*
  - *audio or video products;*
  - *software;*
  - *models;*
  - *educational aids or curricula;*
  - *instruments or equipment;*
  - *research material (e.g., Germplasm; cell lines, DNA probes, animal models);*
  - *clinical interventions;*
  - *new business creation; and*
  - *other.*

Nothing to report.

7. PARTICIPANTS & OTHER COLLABORATING ORGANIZATIONS

What individuals have worked on the project?

Provide the following information for: (1) PDs/PIs; and (2) each person who has worked at least one person month per year on the project during the reporting period, regardless of the source of compensation (a person month equals approximately 160 hours of effort). If information is unchanged from a previous submission, provide the name only and indicate "no change."

Name: *Himisha Beltran, MD*
Project Role: *PI*
Researcher Identifier (e.g. ORCID ID):
Nearest person month worked:

Contribution to Project: *Work on Aim 1,2,3*
Funding Support:

Name: *David Rickman, PhD*
Project Role: *PI*
Researcher Identifier (e.g. ORCID ID):
Nearest person month worked: *3*

Contribution to Project:	*Work on Aim 1,2,3*
Funding Support:	

Name:	*Brian Robinson, MD*
Project Role:	*co-I*
Researcher Identifier (e.g. ORCID ID):	
Nearest person month worked:	

Contribution to Project:	*Work on Aim 1,2*
Funding Support:	

Name:	*Nicholas Brady*
Project Role:	*Post-doctoral fellow*
Researcher Identifier (e.g. ORCID ID):	
Nearest person month worked:	*3*

Contribution to Project:	*Work on Aim 2*
Funding Support:	*This award.*

Has there been a change in the active other support of the PD/PI(s) or senior/key personnel since the last reporting period?

1R01CA230913-01A1 (Rickman)
National Institutes of Health-National Cancer Institute, 2019-2024
Defining Molecular Determinants of Lineage Plasticity as a Mechanism of Treatment Resistance in Prostate Cancer
Roles: PI (Rickman), Co-Investigator (Beltran)
Goals/Aims: To characterize the synergy between *MYCN* induction and *RB1* loss and downstream events that promote lineage switching and treatment response at a single-cell resolution.

1R01CA179100-01A1 (Goodrich)
National Institutes of Health-National Cancer Institute, 2014-2020
NOTCH signaling controls transformation to androgen independent, neuroendocrine prostate cancer."
Role: co-Investigators (Beltran, Rickman)
Goals/Aims: To characterize the NOTCH signaling and its role in the transformation to androgen independent, neuroendocrine prostate cancer.

PC180216 (Barbieri)
Idea Development Award, US Department of Defense, Prostate Cancer Research Program, 2019-2021
Defining the Potential of Early Molecular Subtypes of Prostate Cancer to Progress to AR-Indifferent Disease
Goals/Aims: To define genomic subclasses of early PCa that are susceptible or resistant to conversion to NEPC and to determine if SPOP mutations prevent N-Myc driven conversion to NEPC using unique preclinical platforms.
Role: co-Investigators (Rickman, Beltran)

PC180637 (Giannakakou)
Idea Development Award, US Department of Defense, Prostate Cancer Research Program, 2019-2021.
Transferrin Receptor Identifies a Comprehensive Pool of Circulating Tumor Cells with Unique Molecular Features from Metastatic Prostate Cancer Patients
Goals/Aims: To examine if the transferrin receptor expression is functionally linked with N-Myc and contributes to disease progression and that TfR+-CTC provide for the first time a liquid biopsy approach that can help the diagnosis and molecular characterization of NEPC.
Role: co-Investigators (Beltran, Rickman)

2017 PCF Challenge Award (Zoubeidi / Beltran)
12/31/2017– 12/31/2019
Prostate Cancer Foundation
Targeting BRN2 in Neuroendocrine Prostate Cancer
Goals/Aims: To assess if BRN2 inhibitors should be deployed alone or in combination with current standard-of-care to block the emergence and/or progression of NEPC.

P50 CA211024 Specialized Programs of Research Excellence (SPORE) (Loda)
National Cancer Institute, 08/01/2017-07/30/2022
Weill Cornell Medicine (WCM) SPORE in Prostate Cancer
Project 1: *Non-invasive clinical assay for early detection of treatment resistance in patients with metastatic prostate cancer* (Beltran/Demichelis)
Project 2: *Targeting N-MYC and EZH2-Driven Castrate Resistant Prostate Cancer* (Project Leaders: Rickman / Beltran)
Effort: 1.2 calendar (Project 1); 1.2 calendar (Project 2)
Goals/Aims Project 1: The goals of this project are to determine tumor dynamics and the clinical impact of circulating alterations in predicting response to AR-directed therapy and define the spectrum of circulating DNA alterations in patients with metastatic CRPC.
Goals/Aims Project 2: The goal of this project is to develop more effective targeting strategies for a biomarker-selected subgroup of late stage CRPC driven by N-Myc and less dependent on the AR.

8. SPECIAL REPORTING REQUIREMENTS

COLLABORATIVE AWARDS: For collaborative awards, independent reports are required from BOTH the Initiating PI and the Collaborating/Partnering PI. A duplicative report is acceptable; however, tasks shall be clearly marked with the responsible PI and research site. A report shall be submitted to **https://ers.amedd.army.mil** for each unique award.

QUAD CHARTS: If applicable, the Quad Chart (available on https://www.usamraa.army.mil) should be updated and submitted with attachments.

9. APPENDICES:

Attach all appendices that contain information that supplements, clarifies or supports the text. Examples include original copies of journal articles, reprints of manuscripts and abstracts, a curriculum vitae, patent applications, study questionnaires, and surveys, etc.